

Deep learning algorithm for core-collapse supernova detection

Irene Di Palma

University of Rome Sapienza and INFN

Irene.DiPalma@roma1.infn.it

December 1, 2021




AMALDI
RESEARCH CENTER



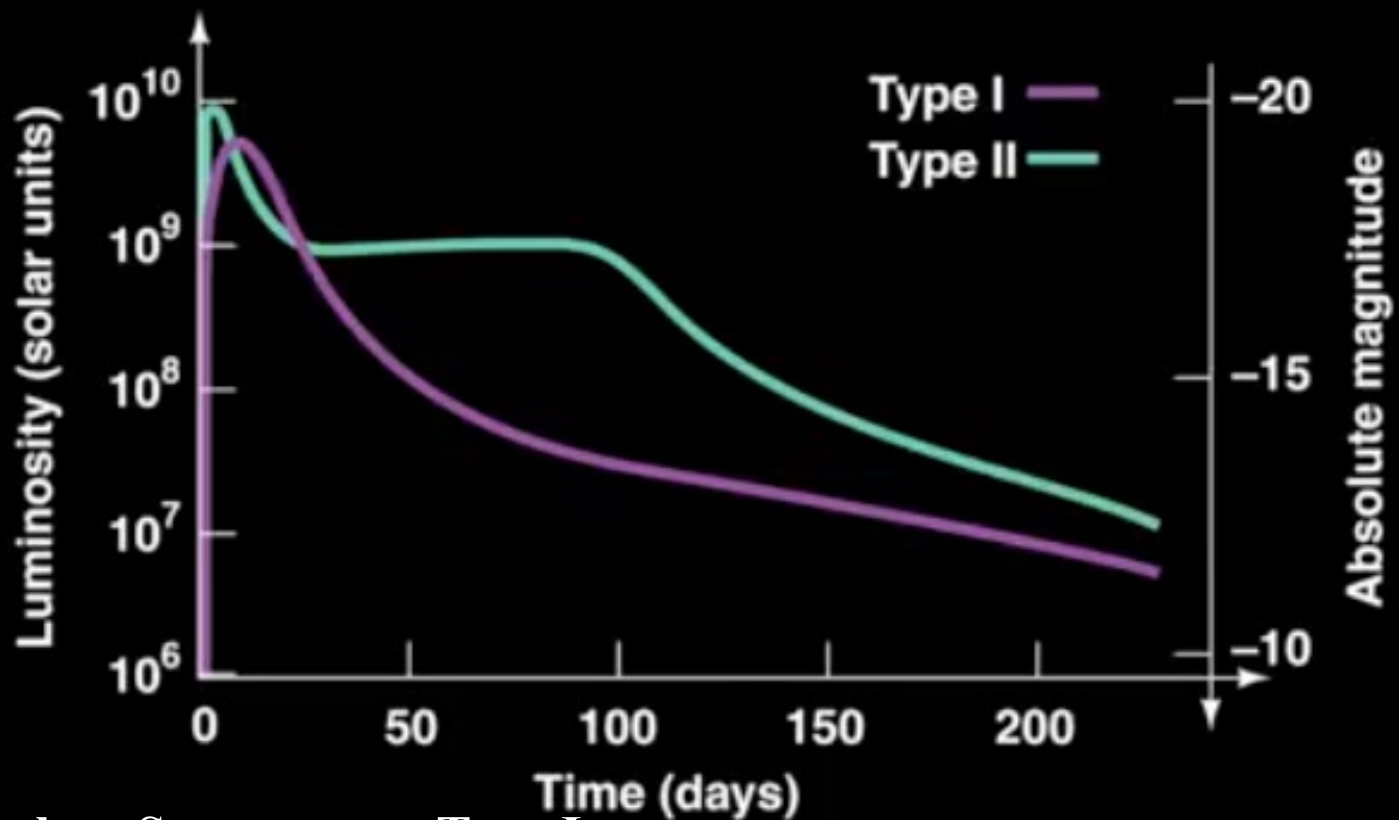
Outline

- What is the astrophysical source we are looking for?
- What are the challenges?
- How do we approach the problem?
- How can we improve our approach?



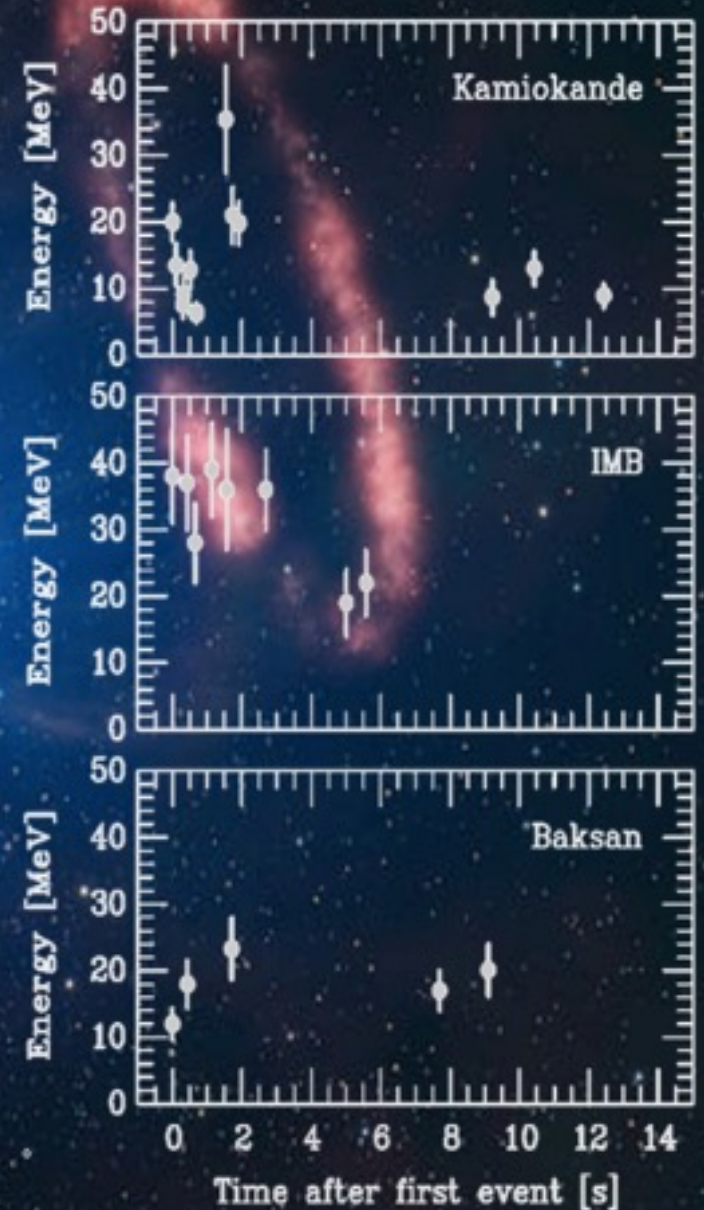
~1 SN / sec in the Universe.
~1 SN / day discovered
(many discovered by amateur astronomers!).
~1 SN / 30-50 years in the Milky Way.

Supernova (SN) 1994D



- **Thermonuclear Supernovae: Type Ia**
 - Caused by runaway thermonuclear burning of white dwarf fuel to Nickel
 - Roughly of 10^{51} ergs released
 - Very bright, used as standard candles
 - No remnant
- **Core Collapse Supernovae: Type II, Ib, Ic**
 - Result from the collapse of an iron core in an evolved massive star ($M_{\text{ZAMS}} > 8-10 M_{\text{SUN}}$)
 - Few $\times 10^{53}$ ergs released in gravitational collapse, most (99%) radiated in neutrinos
 - Spread stellar evolution elemental products throughout galaxy
 - Neutron star or black hole remnant

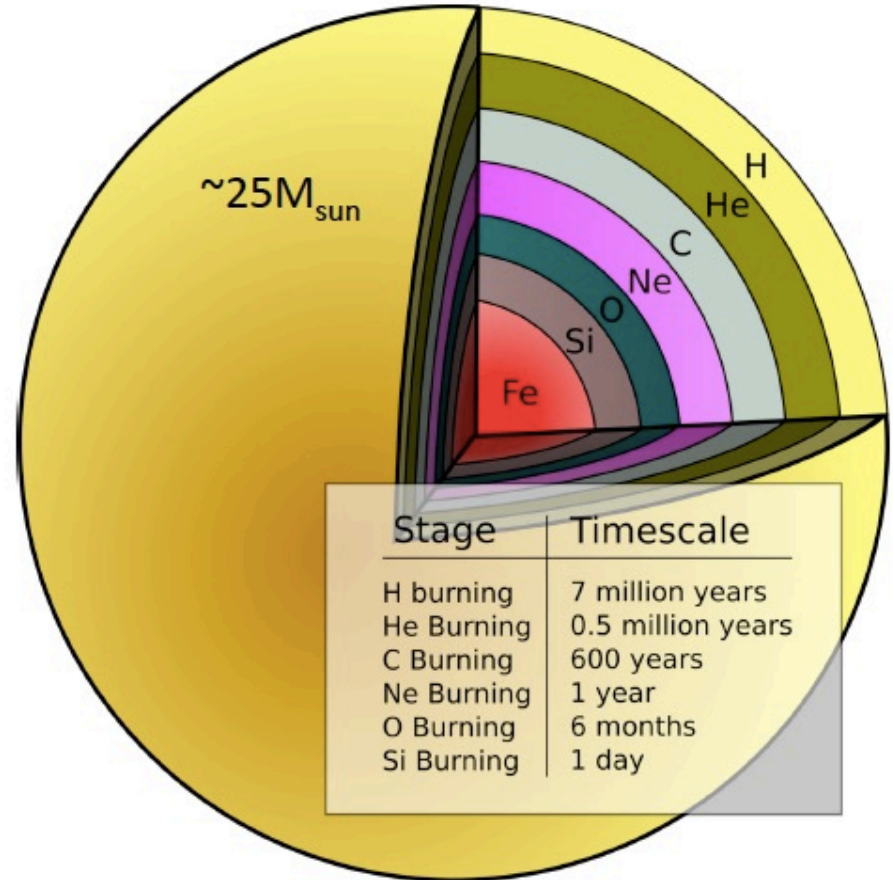
MeV Neutrinos from SN1987A



February 23, 1987.

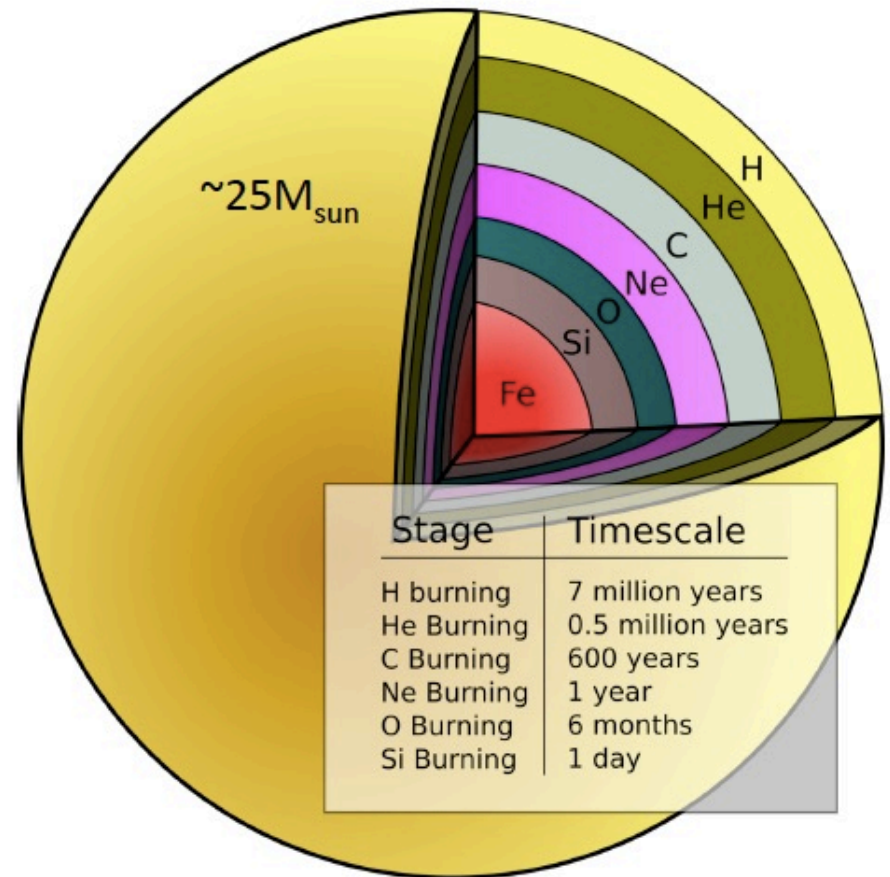
Massive Stars: Burning stages

- Stars spend most of their lives burning hydrogen.
- The product – helium – settles in the core and will burn when temperatures increase sufficiently.
- For massive stars ($M > 8-10M_{\text{sun}}$), the process continues through carbon, oxygen, ... , up to iron.
- This process does not continue past iron as iron is one of the most tightly bound nuclei.
- Iron core builds up in center of star.



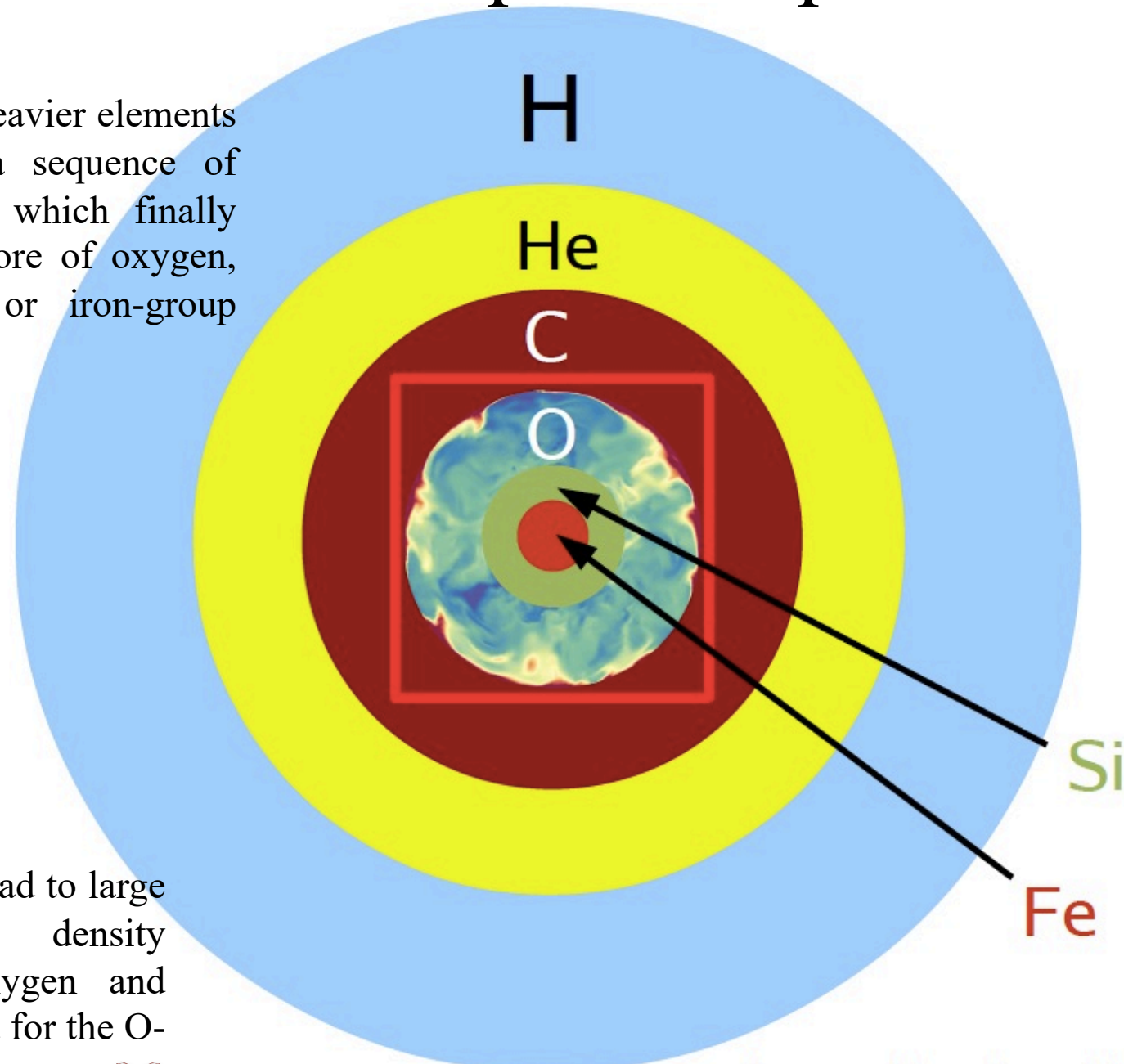
Massive Stars: End Stage

- Stars are, for the majority of the time, in hydrostatic equilibrium because the radiation pressure of the photons from nuclear reactions balance gravity.
- Iron cores however are supported by electron degeneracy pressure, much like a white dwarf, there is a maximum mass that electron degeneracy pressure can support.



Onion shell structure of pre-collapse star

Shells of progressively heavier elements contain the ashes of a sequence of nuclear burning stages, which finally build up a degenerate core of oxygen, neon and magnesium or iron-group elements at the center.

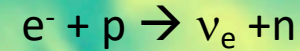


Convective burning can lead to large scale velocity and density perturbations in the oxygen and silicon layers (as indicated for the O-shell).

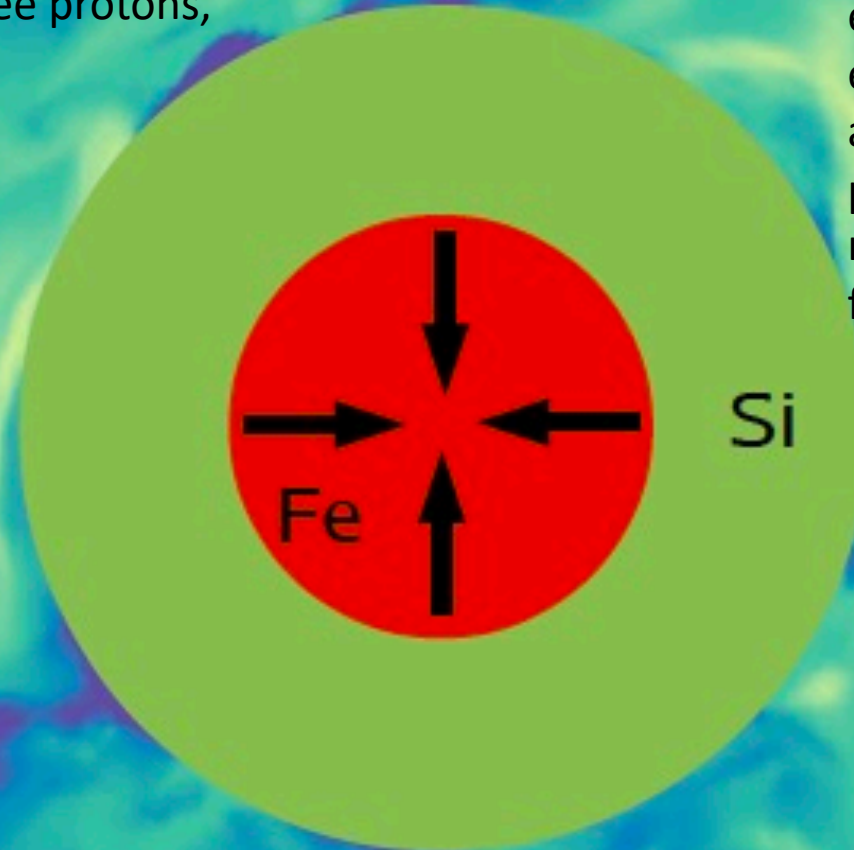


Gravitational instability of stellar core

The gravitational instability of the degenerate O-Ne-Mg or iron core is initiated by electron captures on nuclei and free protons,



and by the partial
photodissociation of heavy
nuclei to α particles and
free nucleons

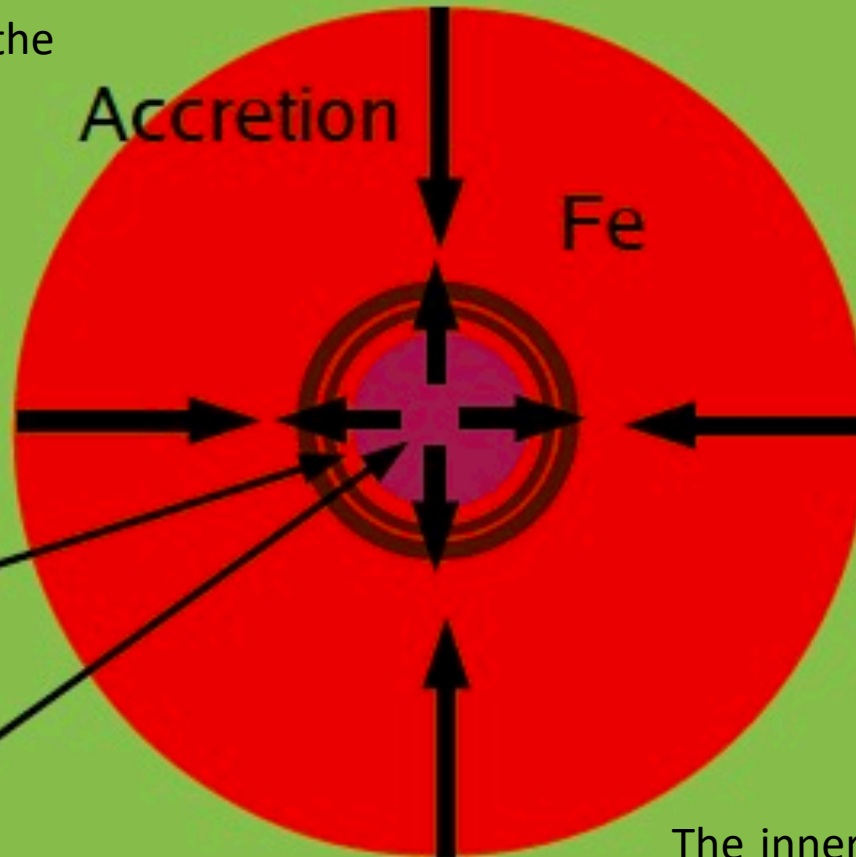


Initially, the electron neutrinos (ν_e) produced by electron captures can escape freely, but at a density of about $10^{12} \text{ g cm}^{-3}$, the outward neutrino diffusion is slower than the accelerating infall of the stellar plasma, and neutrino trapping sets in.



Core bounce at nuclear density

The implosion of the inner core is stopped abruptly when nuclear saturation density is reached at the center



Shock wave

Proto-neutron star

The inner core bounces back and its expansion creates pressure waves that steepen into a shock front at the transition to the supersonically infalling outer core.

Shock stagnation

Accretion

Si

Fe

n, p

Shock
wave

Proto-neutron star

A luminous flash of ν_e , the so-called shock-breakout neutrino burst, is radiated and takes away additional energy from the postshock layer. Since the velocities everywhere behind the shock become negative, the shock expansion stalls and the shock converts into an accretion shock.

Neutrino heating

Accretion

O

Si

n, p

Si

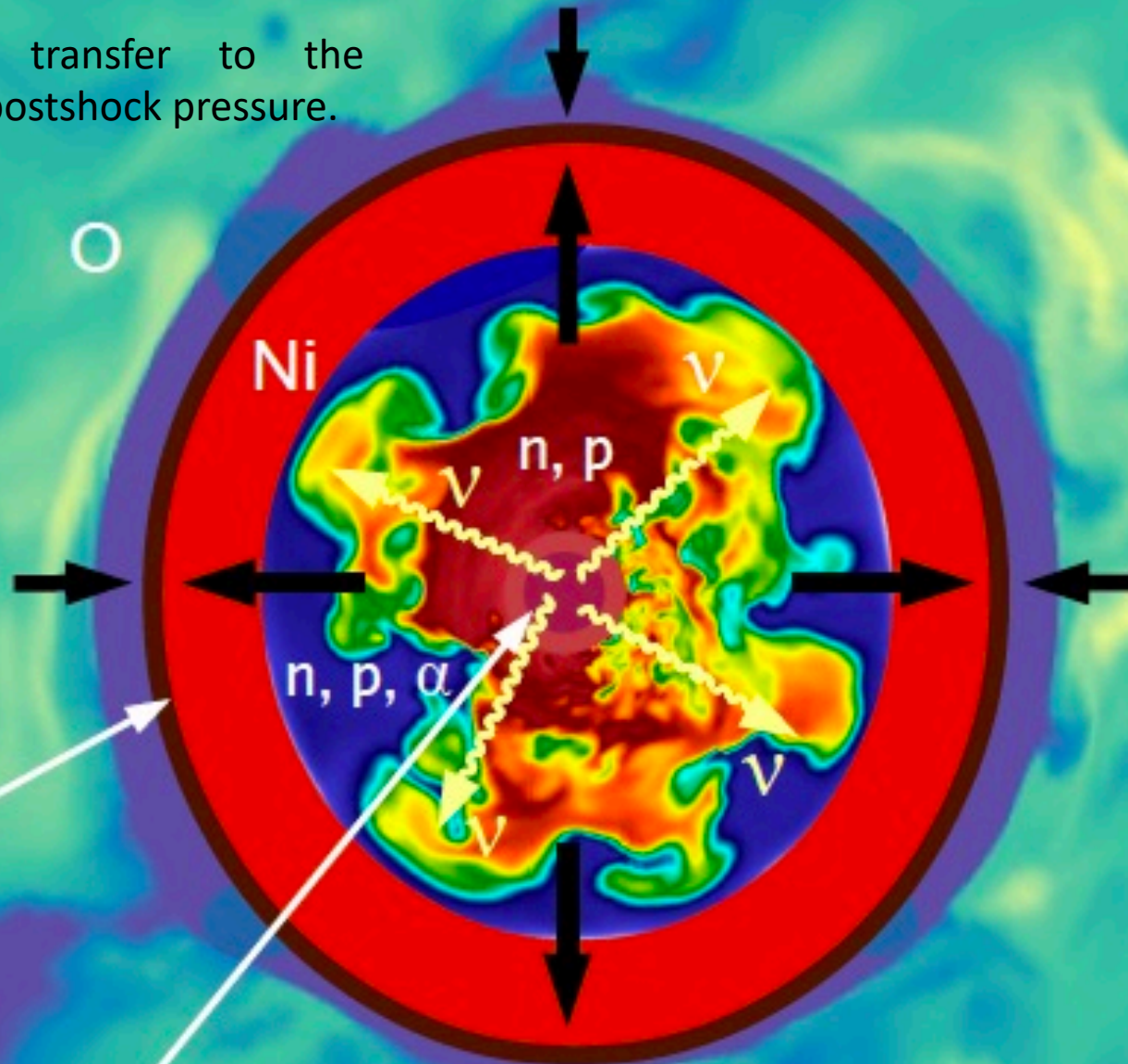
Shock
wave

Proto-neutron star

The conditions, however, change fundamentally at later post-bounce times, because the postshock temperature decreases as the density drops and the plasma becomes more radiation dominated.

Shock revival

Neutrino-energy transfer to the shock raises the postshock pressure.

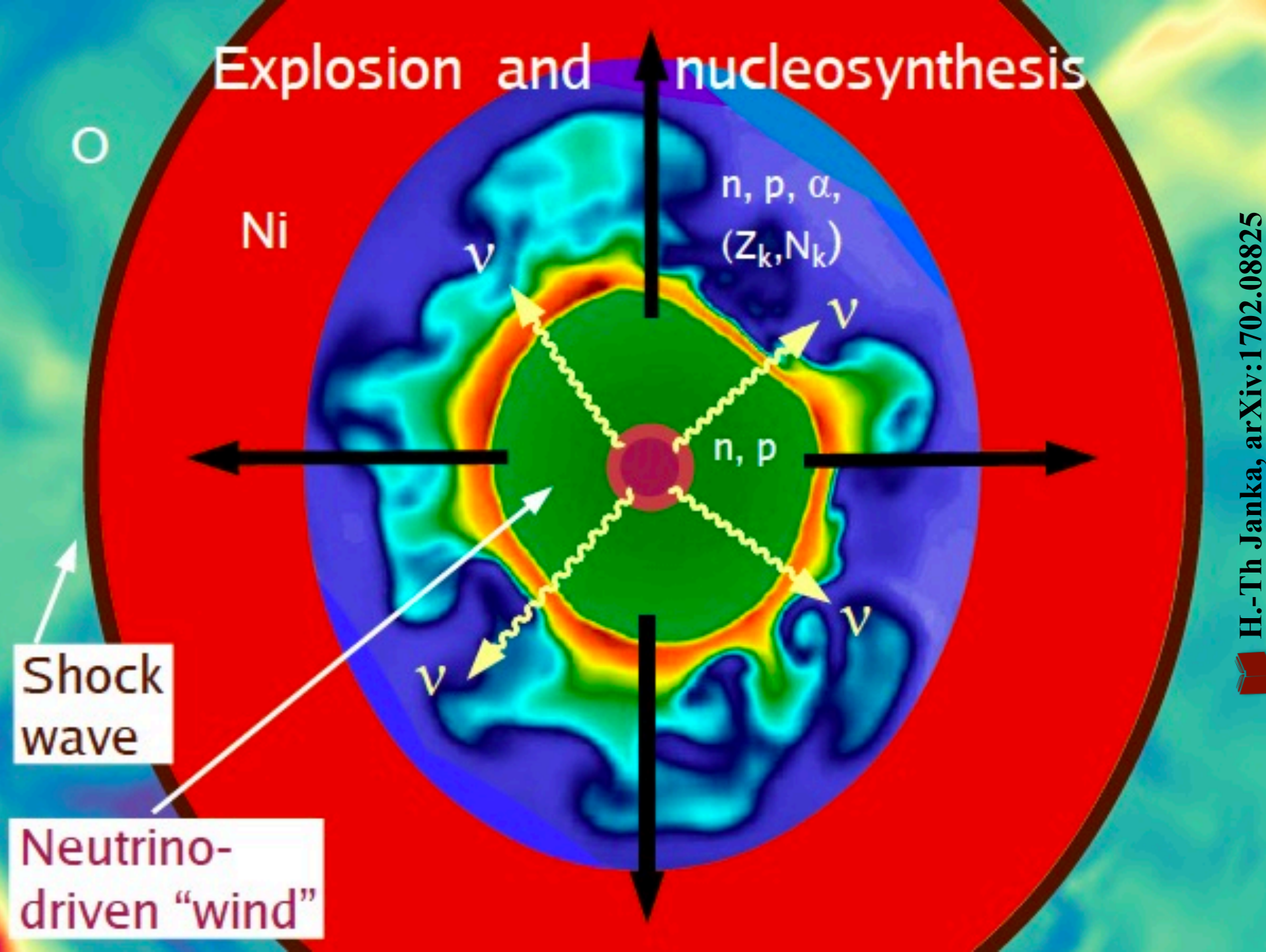


Shock
wave

Proto-neutron star

If the heating by neutrinos is strong enough, the shock can be pushed outwards and the SN explosion can be launched.

Explosion and nucleosynthesis



Outline

- What is the astrophysical source we are looking for?
- **What are the challenges?**
- How do we approach the problem?
- How can we improve our approach?

The challenges

The rate of
observable
CCSN events

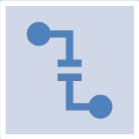
The duty
cycles of the
detectors

The noise
background is
non-stationary

The rates





A neutrino-driven explosion is the most likely outcome in the case of slowly rotating cores, which are present in the bulk of CCSN progenitors. The emitted GWs could be detected with the advanced ground-based GW detector network, Advanced LIGO, Advanced Virgo and KAGRA, within 5 kpc*. Such a galactic event has a rate of about 2-3 per century[#].



For the case of rapidly rotating progenitor cores the result is likely a magnetorotational explosion, yielding a more powerful GW signal that could be detected within 50 kpc.



Despite the low rates, CCSN are of great scientific interest because they produce complex GW signals which could provide significant clues about the physical processes at work after the gravitational collapse of stellar cores.

*  Phys. Rev. D. 93 (2016), 10.1103; Phys. Rev. D. 101, 084002 (2020).
 Astrophys. J. 778, 164 (2013); New Astronomy 83, 101498 (2021).

The duty cycle of the detectors



The fraction of time interferometers are operating and taking science-quality data is limited by several factors including commissioning work (to improve sensitivity and stability) and interference due to excessive environmental noise.



The risk of completely missing a CCSN GW signal is mitigated by having a larger network of detectors.

The noise background is non-stationary





Noise in interferometers arises from a combination of instrumental, environmental, and anthropomorphic noise sources that are extremely difficult to characterize precisely.

Mitigation strategies include:

- Coincident observation with multiple, geographically separated detectors
- Data quality monitoring and the recording of instrumental and environmental vetos derived from auxiliary data channels such as seismometers, magnetometers, etc.
- Glitch-detection strategies based on Bayesian inference^{*} or machine learning[#].
- Using external triggers from EM or neutrino observations to inform the temporal “on-source window” in which we expect to find GW signals and consequently reduce the time period searched.



^{*}  Phys. Rev. D. 82, 103007 (2010); Class. Quantum Grav. 32, 215012 (2015).
[#]  Phys. Rev. D. 88, 062003 (2013).

Outline

- What is the astrophysical source we are looking for?
- What are the challenges?
- **How do we approach the problem?**
- How can we improve our approach?

Motivations

According to the standard paradigm of the neutrino-driven mechanism of the core collapse explosion, the energy transfer by the intense neutrino flux can be the decisive agent for powering the supernova outburst.

In a supernova explosion, also gravitational waves (GW) are generated in the inner core of the source, so that this messenger carries direct information of the inner mechanism.

Although the phenomenon is among of the most energetic in the universe, the amplitude of the gravitational wave impinging on a detector on the Earth is extremely faint.

For a CCSN in the center of the Milky way, a rare event, we could expect amplitudes of the metric tensor perturbations ranging between $10^{-21} - 10^{-23}$.

To increase the event rate of detections we should increase the volume of the universe to be explored and this can be achieved both by decreasing the detector noise and using better performing statistical algorithms.



Deep learning for core-collapse supernova detection

M. López^{1,2,†} I. Di Palma^{3,*} M. Drago^{3,4} P. Cerdá-Durán⁵ and F. Ricci³

The detection of gravitational waves from core-collapse supernova (CCSN) explosions is a challenging task, yet to be achieved, in which it is key the connection between multiple messengers, including neutrinos and electromagnetic signals. In this work, we present a method for detecting these kind of signals based on machine learning techniques. We tested its robustness by injecting signals in the real noise data taken by the Advanced LIGO-Virgo network during the second observing run, O2. We trained a newly developed Mini-Inception Resnet neural network using time-frequency images corresponding to injections of simulated phenomenological signals, which mimic the waveforms obtained in 3D numerical simulations of CCSNe. With this algorithm we were able to identify signals from both our phenomenological template bank and from actual numerical 3D simulations of CCSNe. We computed the detection efficiency versus the source distance, obtaining that, for signal to noise ratio higher than 15, the detection efficiency is 70% at a false alarm rate lower than 5%. We notice also that, in the case of the O2 run, it would have been possible to detect signals emitted at 1 kpc of distance, while lowering down the efficiency to 60%, the event distance reaches values up to 14 kpc.

DOI: [10.1103/PhysRevD.103.063011](https://doi.org/10.1103/PhysRevD.103.063011)



A NEW GRAVITATIONAL-WAVE SIGNATURE FROM STANDING ACCRETION SHOCK INSTABILITIES IN SUPERNOVAE

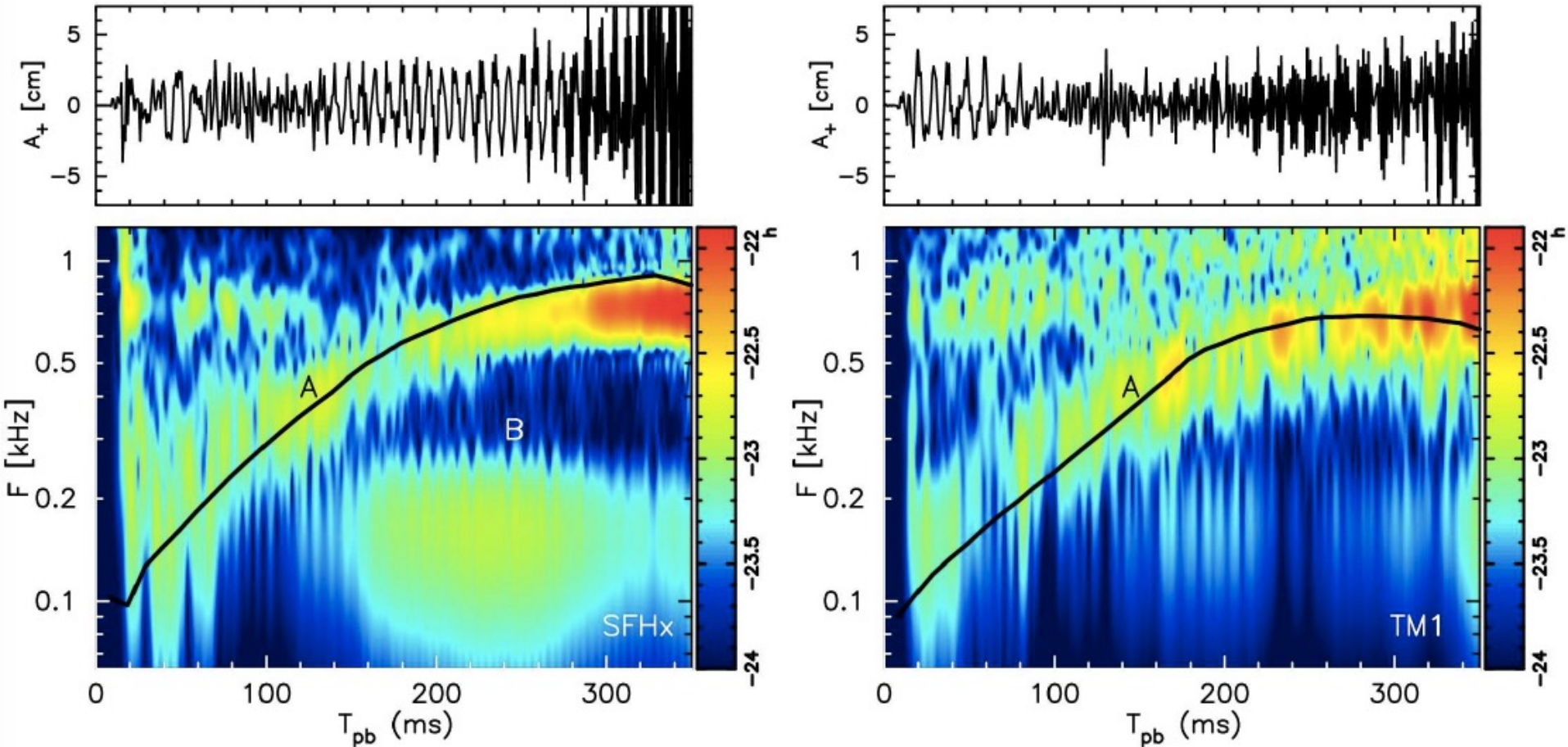
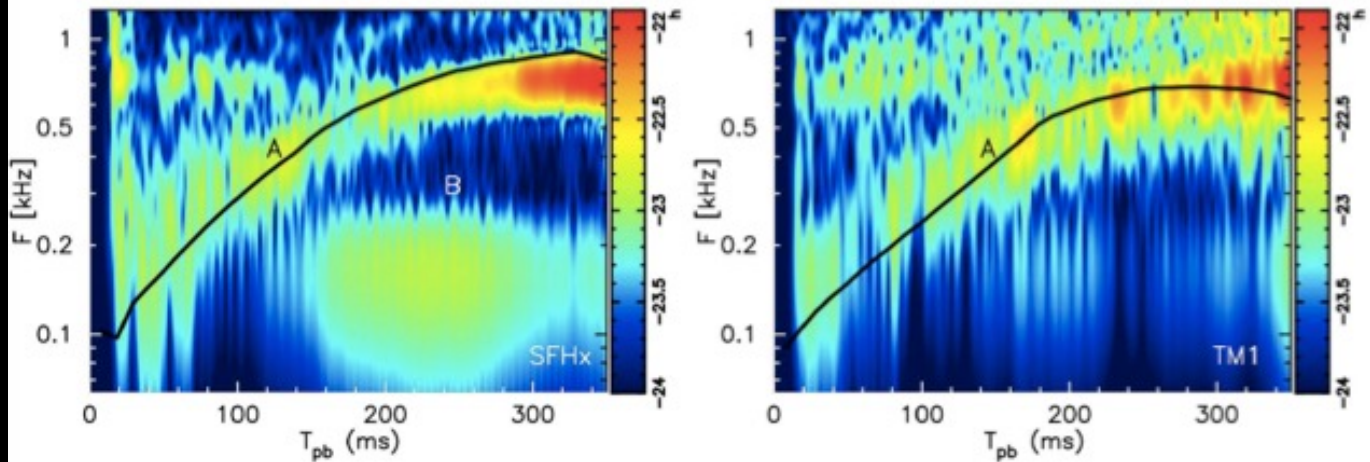


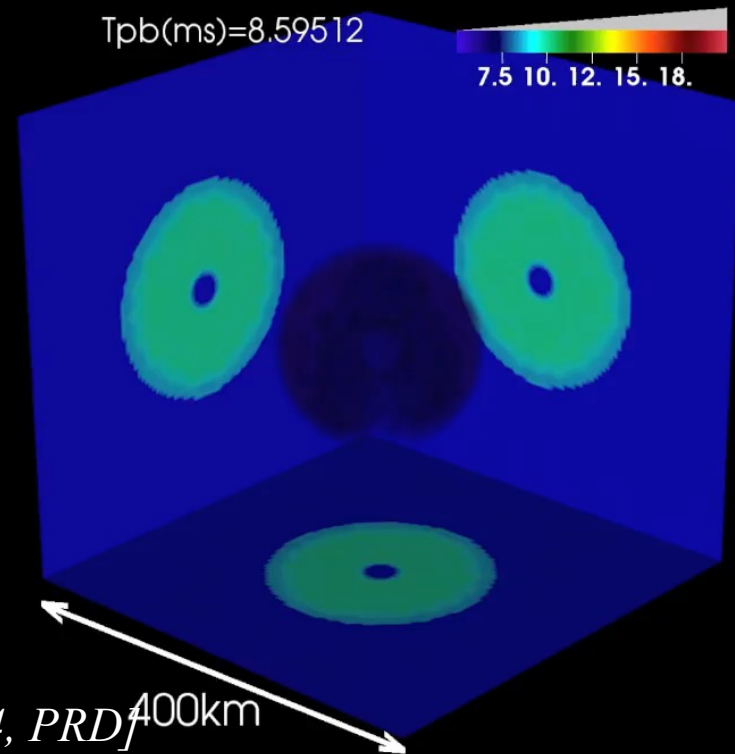
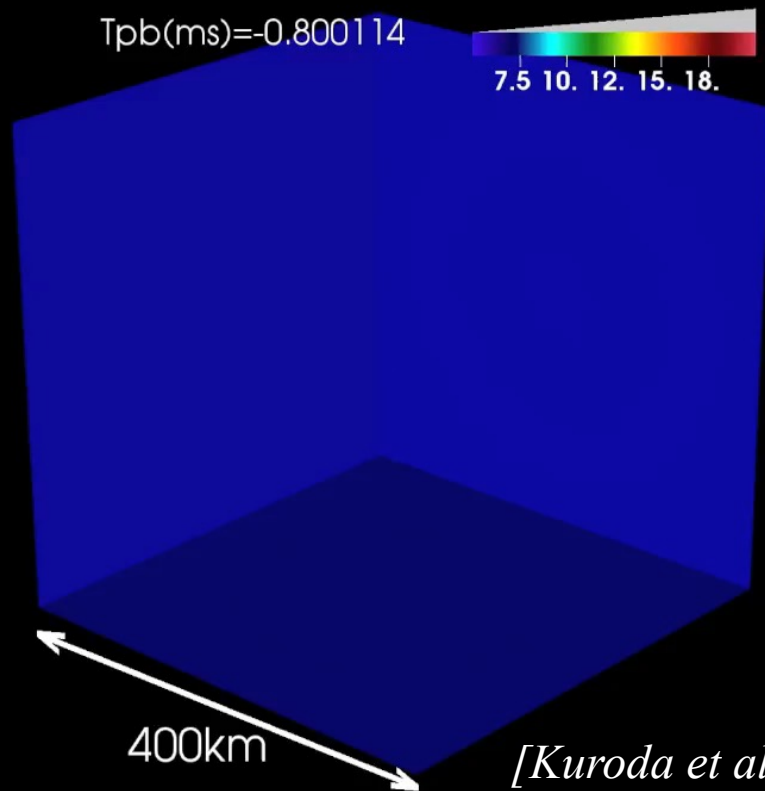
FIG. 1.— In each set of panels, we plot, top; gravitational wave amplitude of plus mode A_+ [cm], bottom; the characteristic wave strain in frequency-time domain \tilde{h} in a logarithmic scale which is over plotted by the expected peak frequency F_{peak} (black line denoted by “A”). “B” indicates the low frequency component. The component “A” is originated from the PNS g -mode oscillation (Marek & Janka 2009; Müller et al. 2013). The component “B” is considered to be associated with the SASI activities (see Sec. 3). Left and right panels are for TM1 and SFHx, respectively. We mention that SFHx (left) and TM1 (right) are softer and stiffer EoS models, respectively. 23





SFHx :softer

TM1 :stiffer

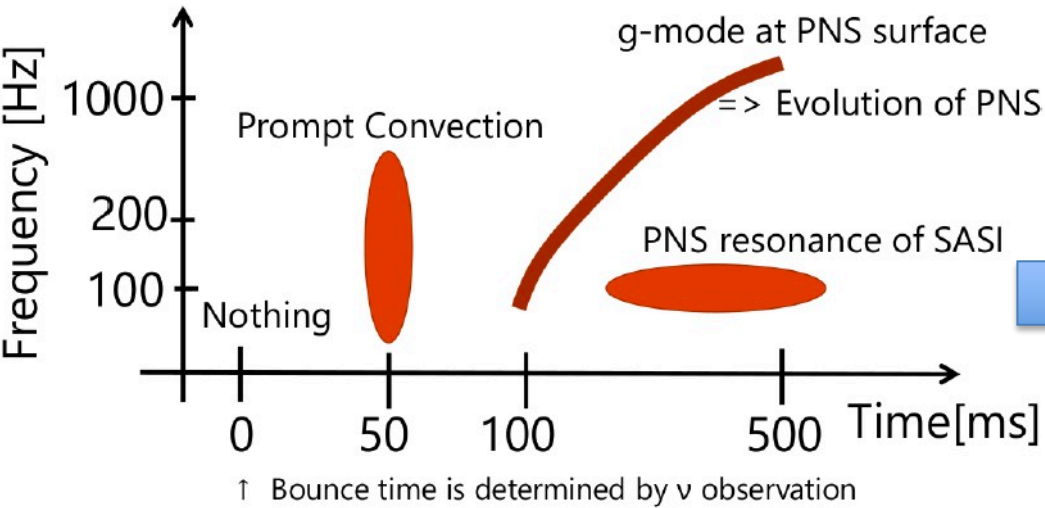


[Kuroda et al 2016, ApJL, 2014, PRD]

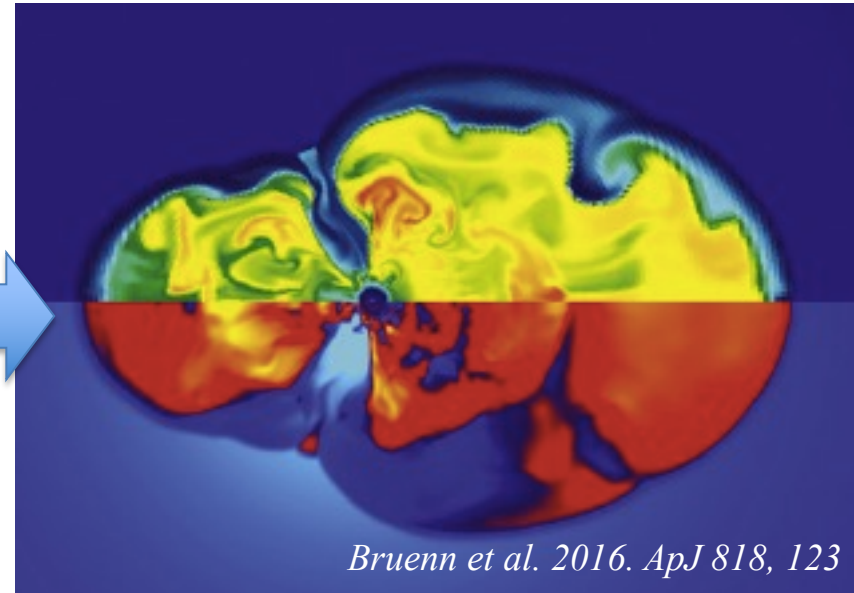
✓ **SASI activity higher for softer EOS** (due to high growth rate, e.g., Foglizzo et al. ('06)).

Different scenarios

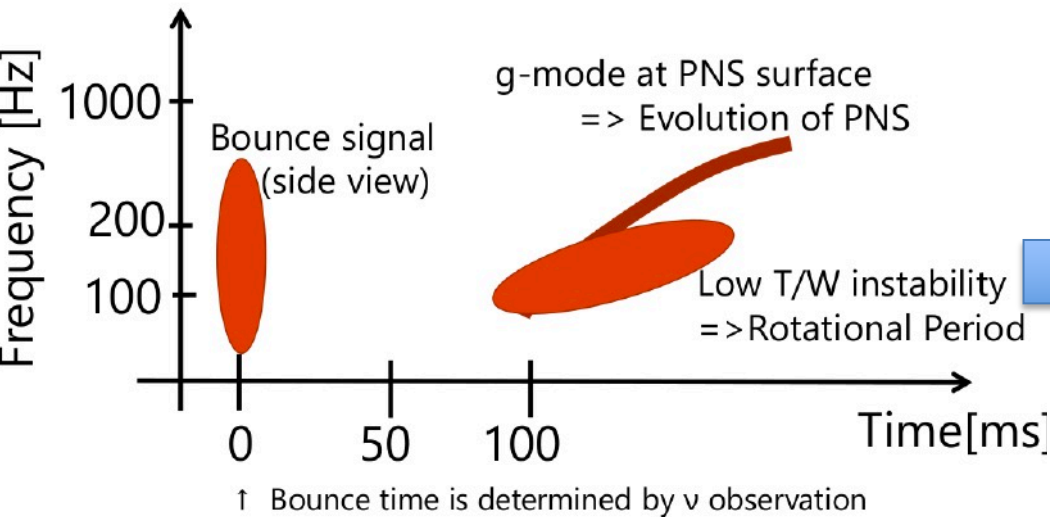
Non rotating scenario



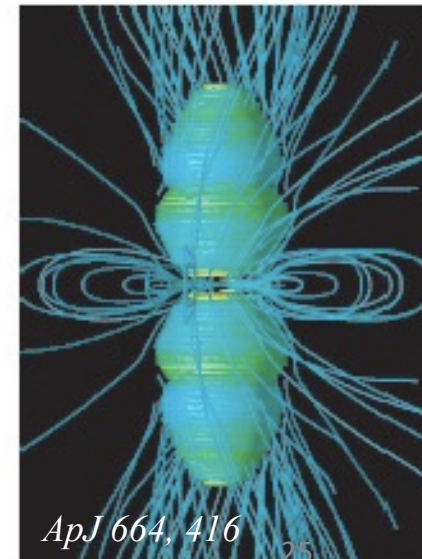
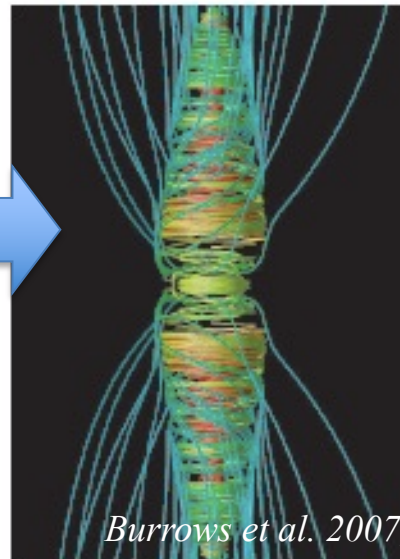
Neutrino driven CCSNe



Rapidly rotating scenario



Magneto-rotationally-driven CCSNe



Credit: Tomoya Takiwaki

Phenomenological Waveforms

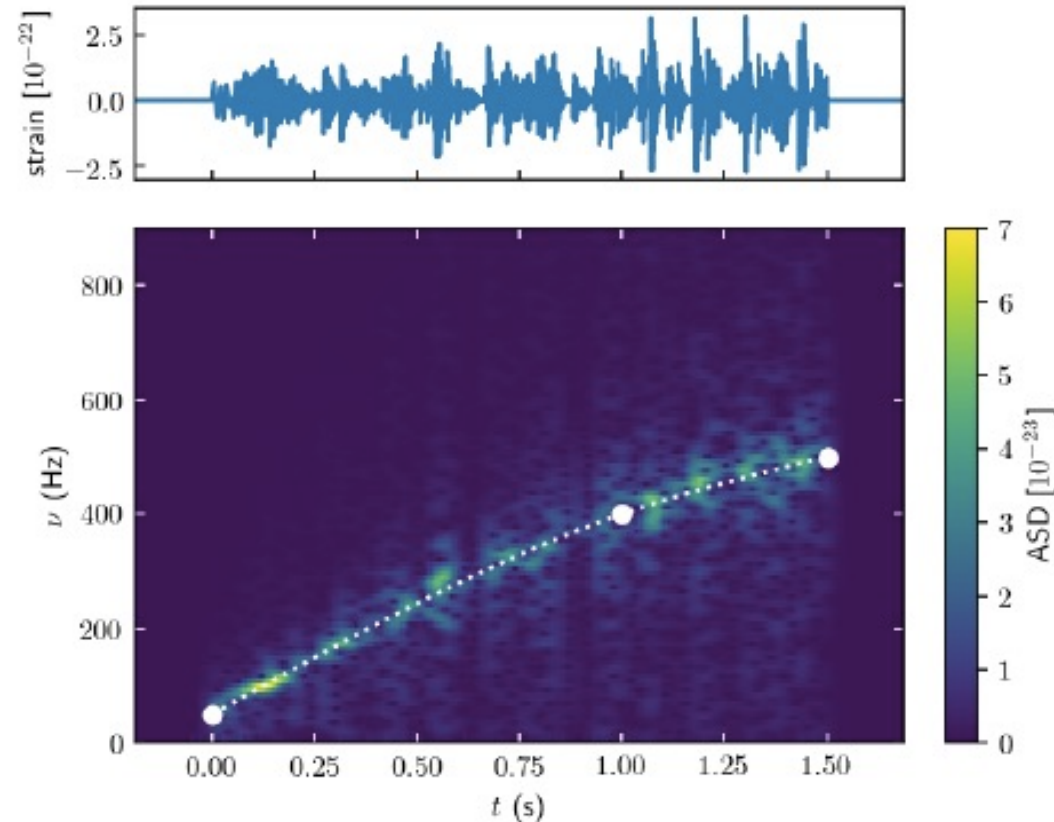
The aim of our phenomenological template is to mimic the raising arch observed in core-collapse simulations.

The idea is that at each time in the post-bounce evolution, the PNS is in quasi-hydrostatic equilibrium and any perturbation will excite the eigenmodes of the system, in particular g-modes.

These modes are continually being excited by the hot bubble surrounding the PNS, in particular by convective motions and SASI. At the same time these excited modes are damped by the PNS conditions (e.g. by the existence of convective layers that do not allow for buoyantly supported waves) and by the presence of non-linearities and instabilities (e.g. turbulence).

The GW emission can be modelled as a damped harmonic oscillator with a random forcing, in which the frequency varies with time.

Phenomenological Waveforms



parameter	min.	max.	Δ	description
t_{ini} [s]	0	0.2	0.1	beginning of the waveform
t_{end} [s]	0.2	1.5	0.1	end of the waveform
ν_0 [Hz]	50	150	50	frequency at bounce
ν_1 [Hz]	1000	2000	500	frequency at 1 s
ν_2 [Hz]	1500	4500	1000	frequency at 1.5 s
ν_{driver} [Hz]	100	200	100	driver frequency
Q	(1, 5, 10)			quality factor
D [kpc]	(1, 2, 5, 10, 15)			distance to source

- New and flexible parametrisation for the frequency evolution.
- The distance is used as a parameter.



Strategy



While the neutrino information are used as an external trigger, it is necessary the generation of a data set of CCSN waveforms through a phenomenological approach.



Creation of the time-frequency plots that are the input for the deep learning algorithm.



Analysis of these images through the neural network.



Classification of images as signal or noise.

Gravitational Wave Observatories



LIGO, Livingston, LA



LIGO, Hanford, WA



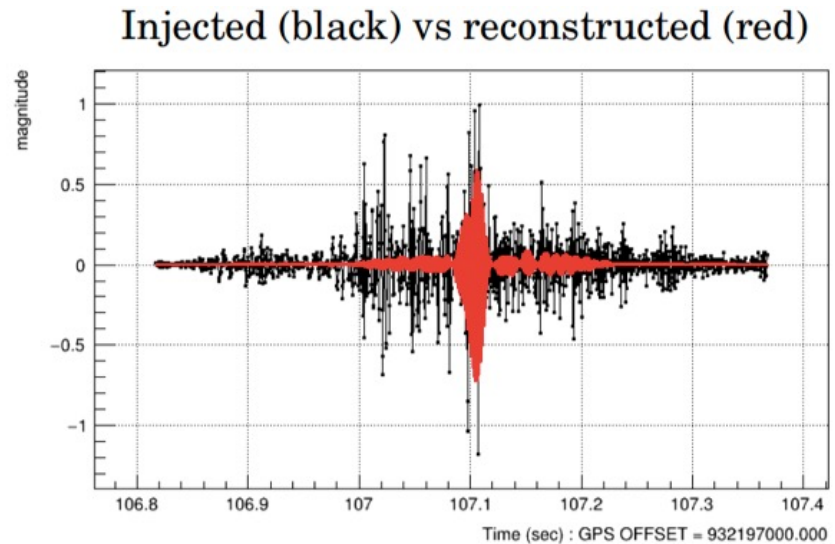
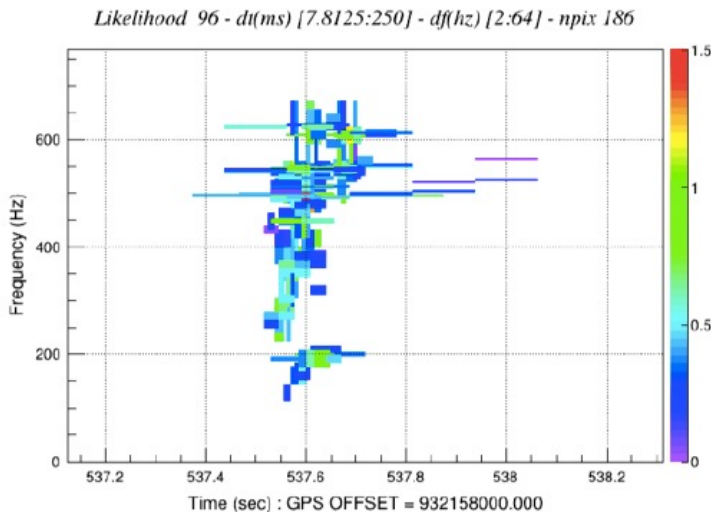
Virgo, Cascina, Italy



KAGRA, Gifu, Japan

Coherent Waveburst (cWB)

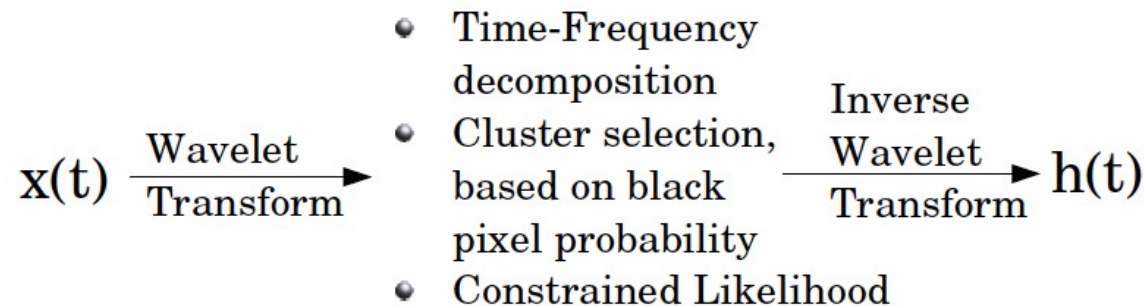
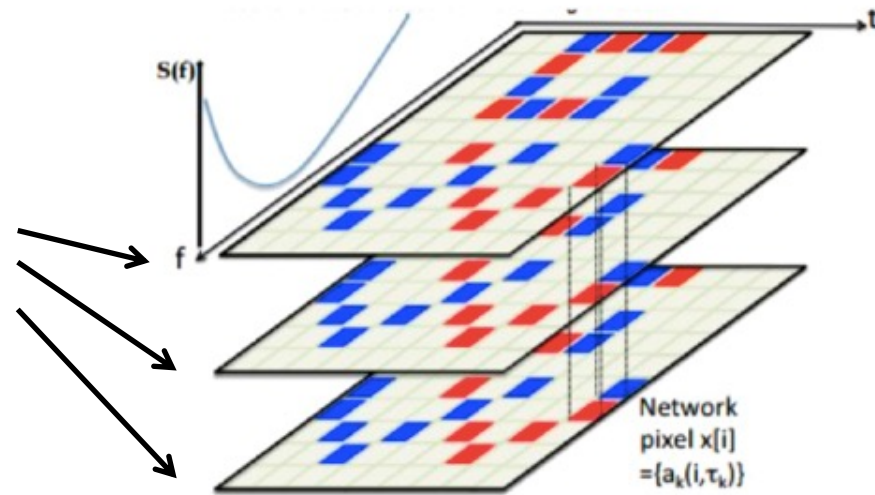
- Coherent Waveburst is an algorithm of Burst search developed at LVC
- Interesting features:
 - Characterization of signal both in time and frequency (Wavelet)
 - Coherent analysis (Likelihood approach)
 - Reconstruction of waveforms and source coordinates
- Waveburst is applied in two steps:
 - **Production**: production events list
 - **Post production**: candidate selection



Coherent Waveburst

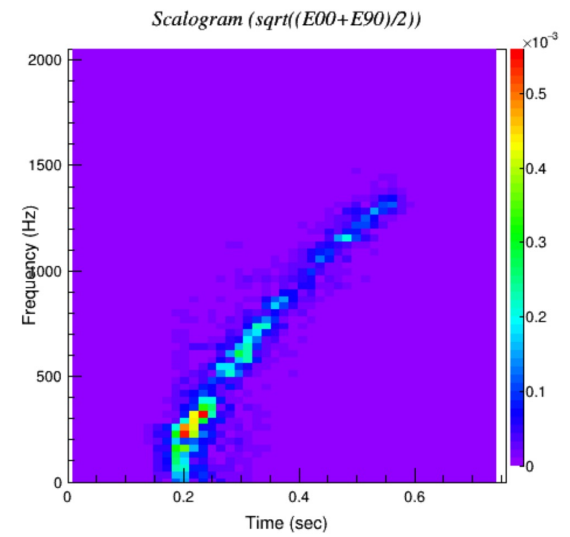
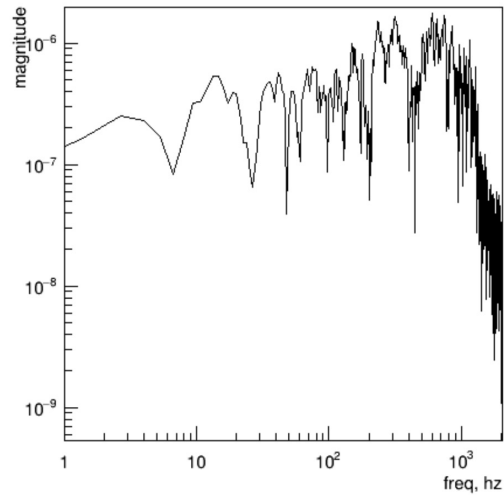
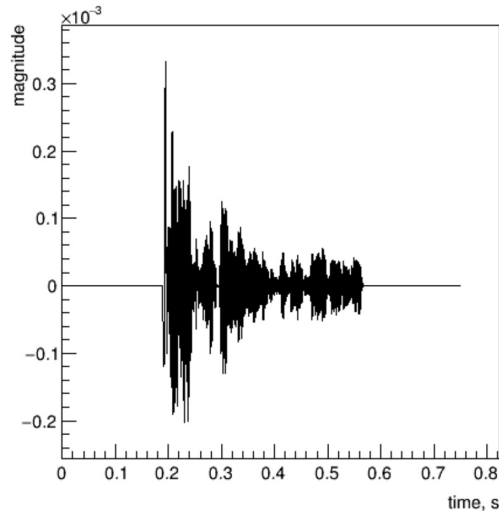
- The pipeline decomposes the data stream, of each detector in the network, at different (dt, df) resolution levels.
- cWB is an Excess power algorithm: minimal assumption on target signal.
- The TF decomposition of the whitened data at a chosen level is considered as input for the neural network.

Representation of
multilayer decomposition
of the GW data

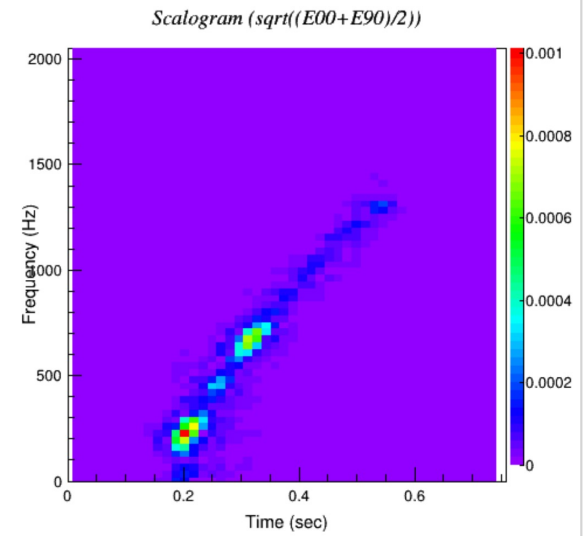
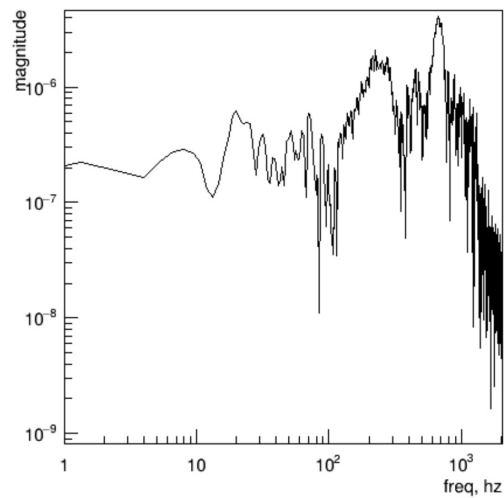
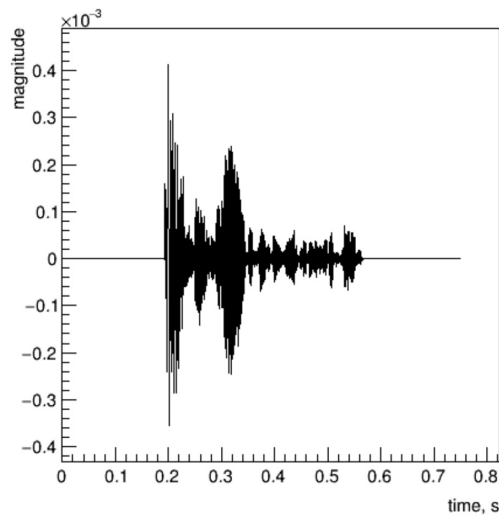


Examples of injections

gw000



gw001



Artificial Neural Network

- What are they?

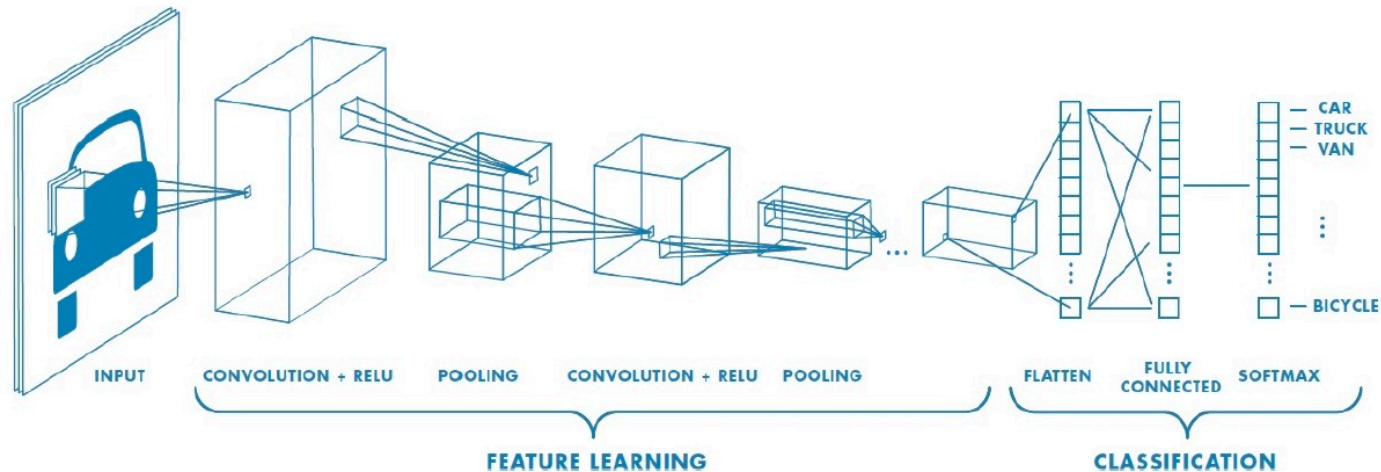
An artificial neural network (ANN) is a mathematical object composed of many layers. Those layers are both linear (convolutions, matrix multiplications) and nonlinear (activation functions, poolings). The network has a multiscale hierarchical structure that is able to describe and combine features at different scales.

- How do they work?

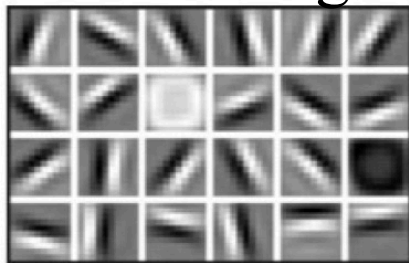
The weights of the network are iteratively updated using a gradient-descent algorithm, trying to minimize an appropriate cost function. Our cost function, the cross-entropy, is related to the classification error.

Convolutional Neural Network

- Convolutional Neural Networks (CNN) are a biologically-inspired trainable architecture that can learn multi-scale hierarchical features.



- This data-driven filter learning provides a visual space decomposition which can be regarded as a hierarchical matched filtering.



First Layer Representation

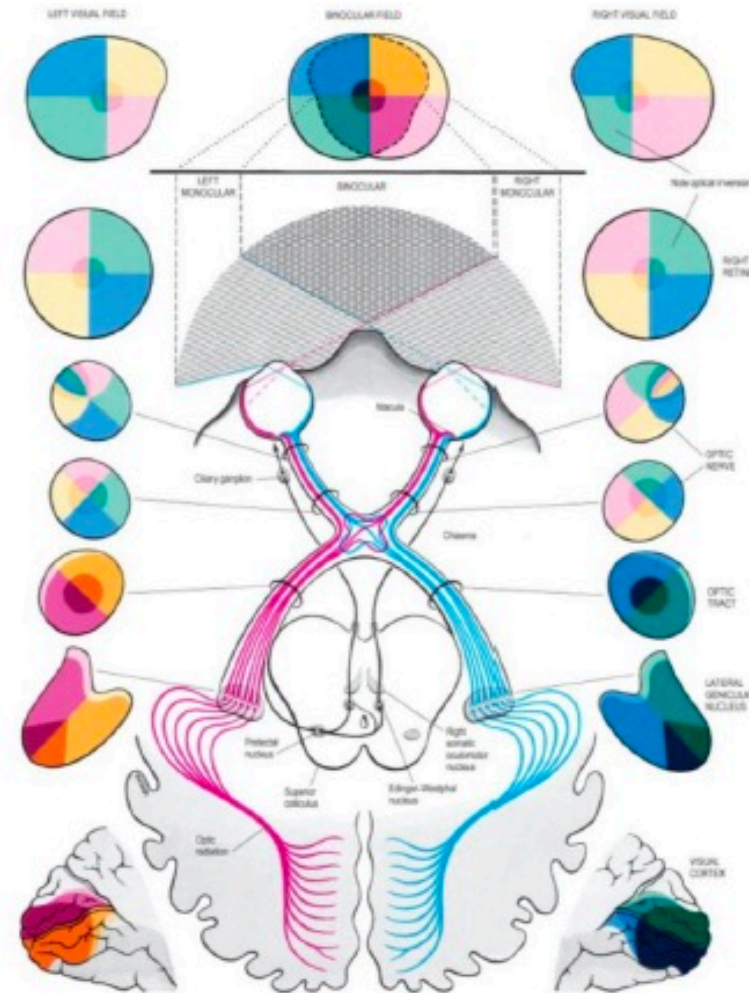
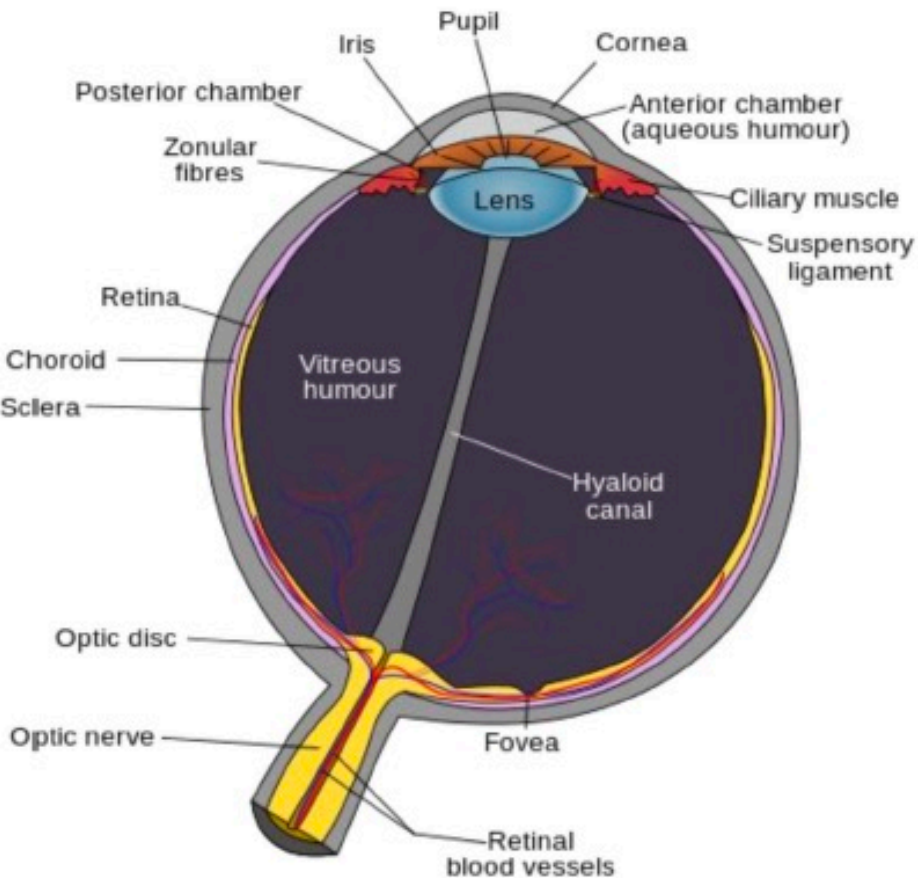


Second Layer Representation



Third Layer Representation

Mimic the brain

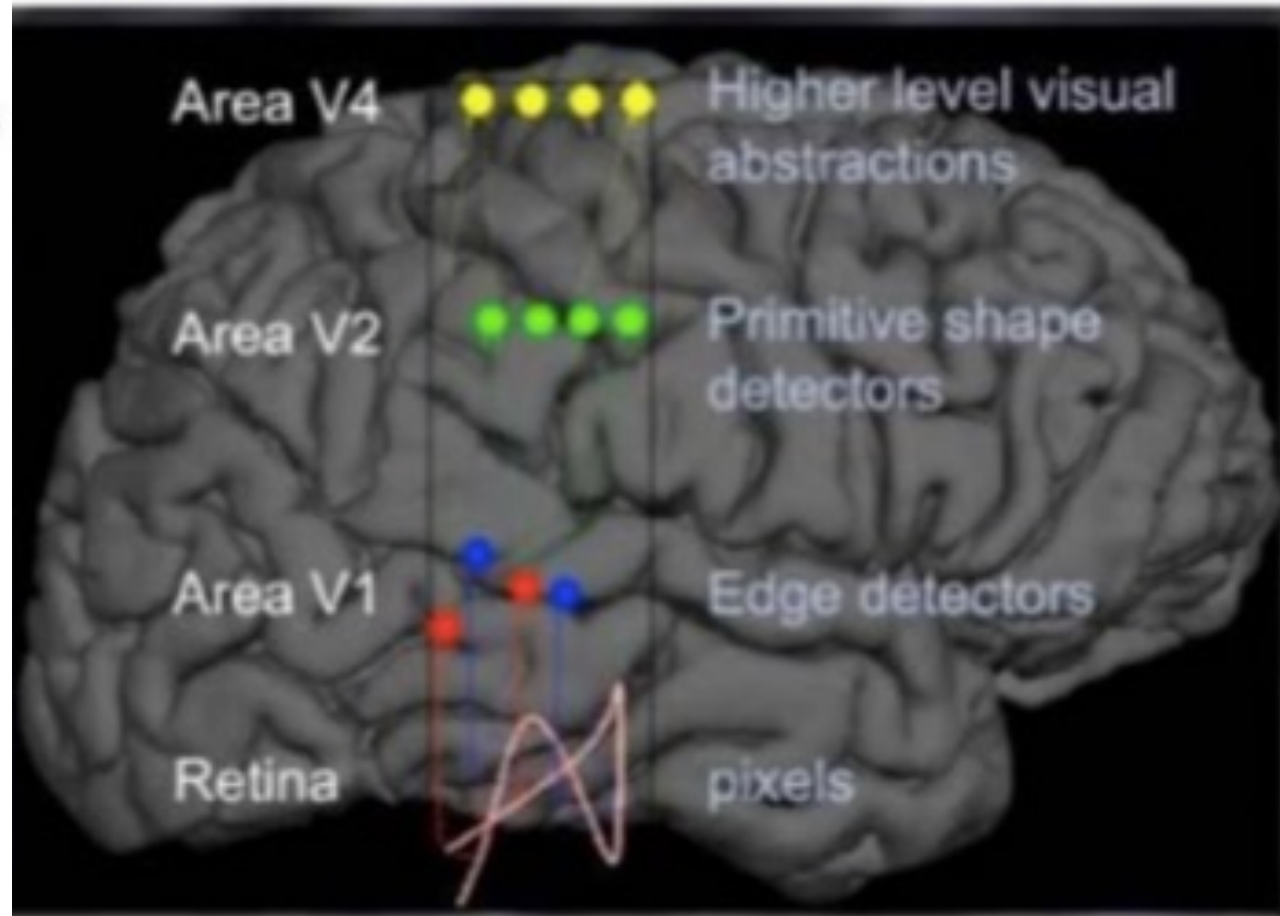
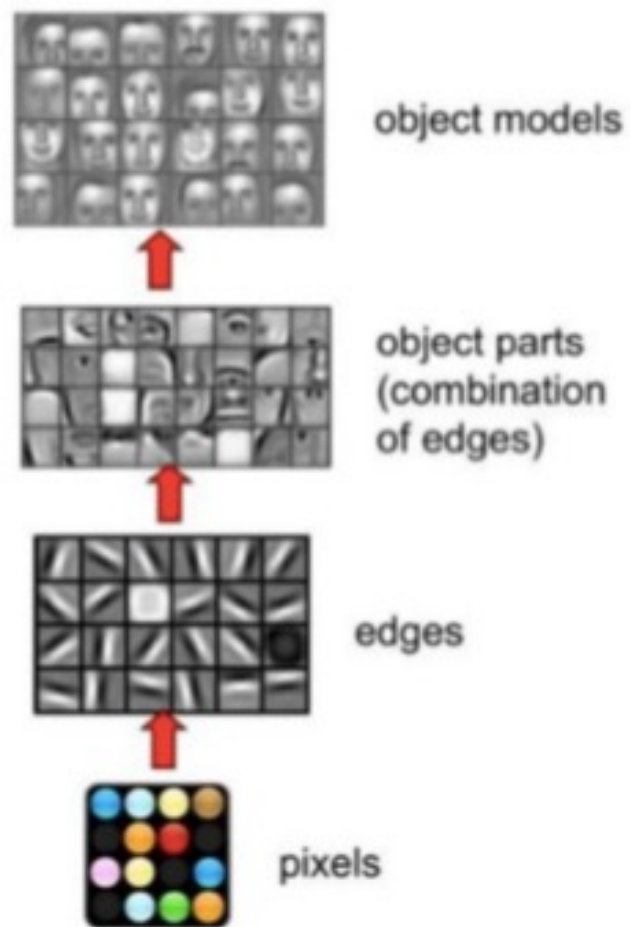


The eye: optical system that creates an upside down image on the retina.

The retina: thin layer of tissue that receives and converts the light into neural signals, and send these signals on to the brain for visual recognition.

The brain: elaborates the data from the retina and builds the final image.

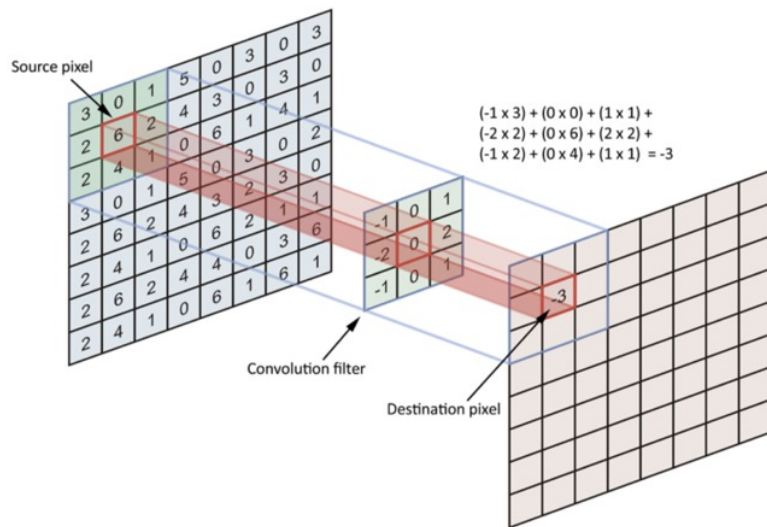
Mimic the brain



Training, Test and Confusion Matrix

The process of achieving the minimisation of the loss function during the **training** stage is the process whereby the machine is “learning”.

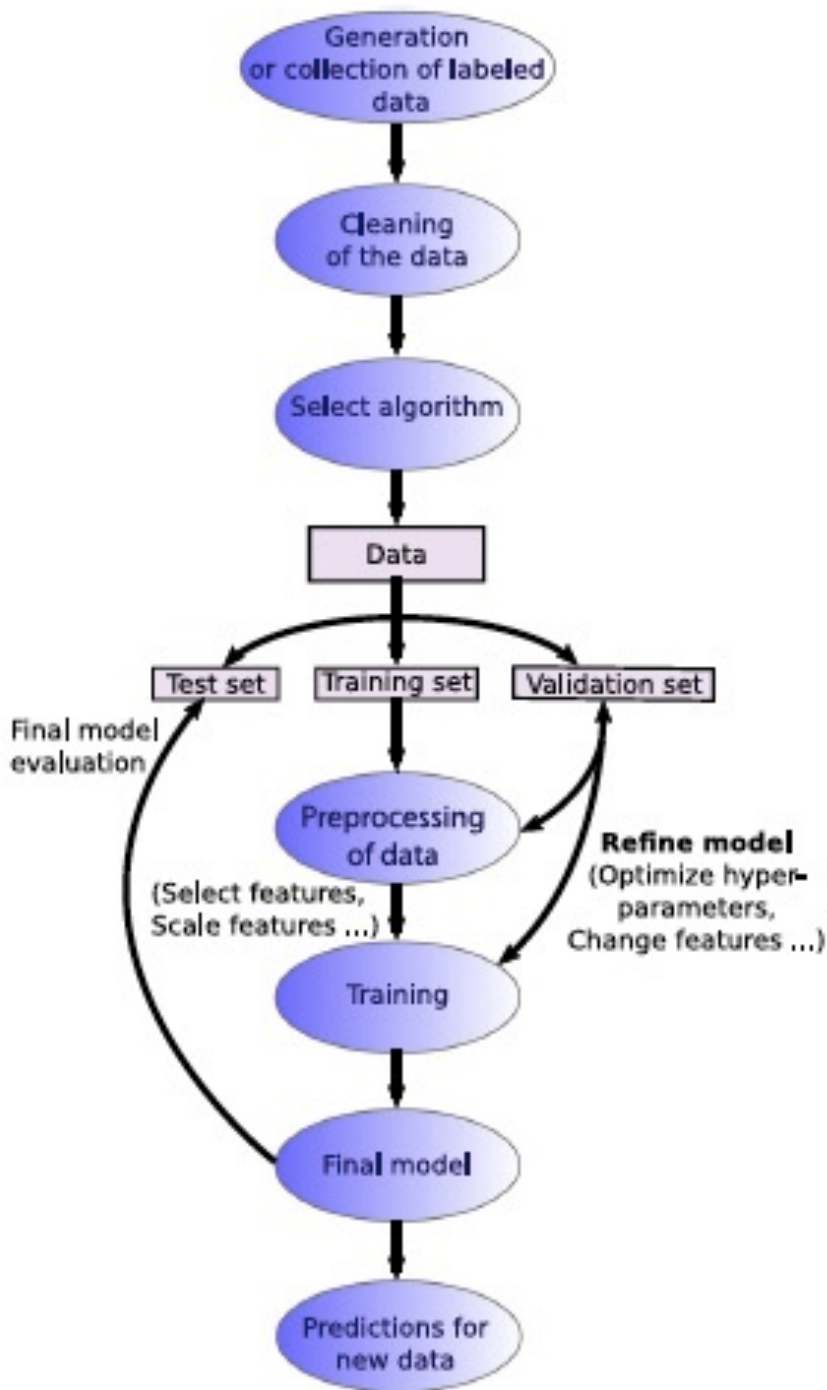
For the **test** stage, the CNN will be able to take in input new data and its output will best represent the probability of that data belonging to each of the trained classes.



The convolution operation.

		Predicted Class	
		Positive	Negative
Actual Class	Positive	True Positive (TP)	False Negative (FN)
	Negative	False Positive (FP)	True Negative (TN)

Supervised learning workflow



Generate/find, and cleaning the data to ensure that they are consistent and accurate.



Decide how to map the properties of the system; this implies to translate the raw information into certain features that will be used as inputs for the algorithm.



The data are split into various sets: a training set, a validation dataset and the test set.



The model is trained by optimizing its performance, measured through the cost function.



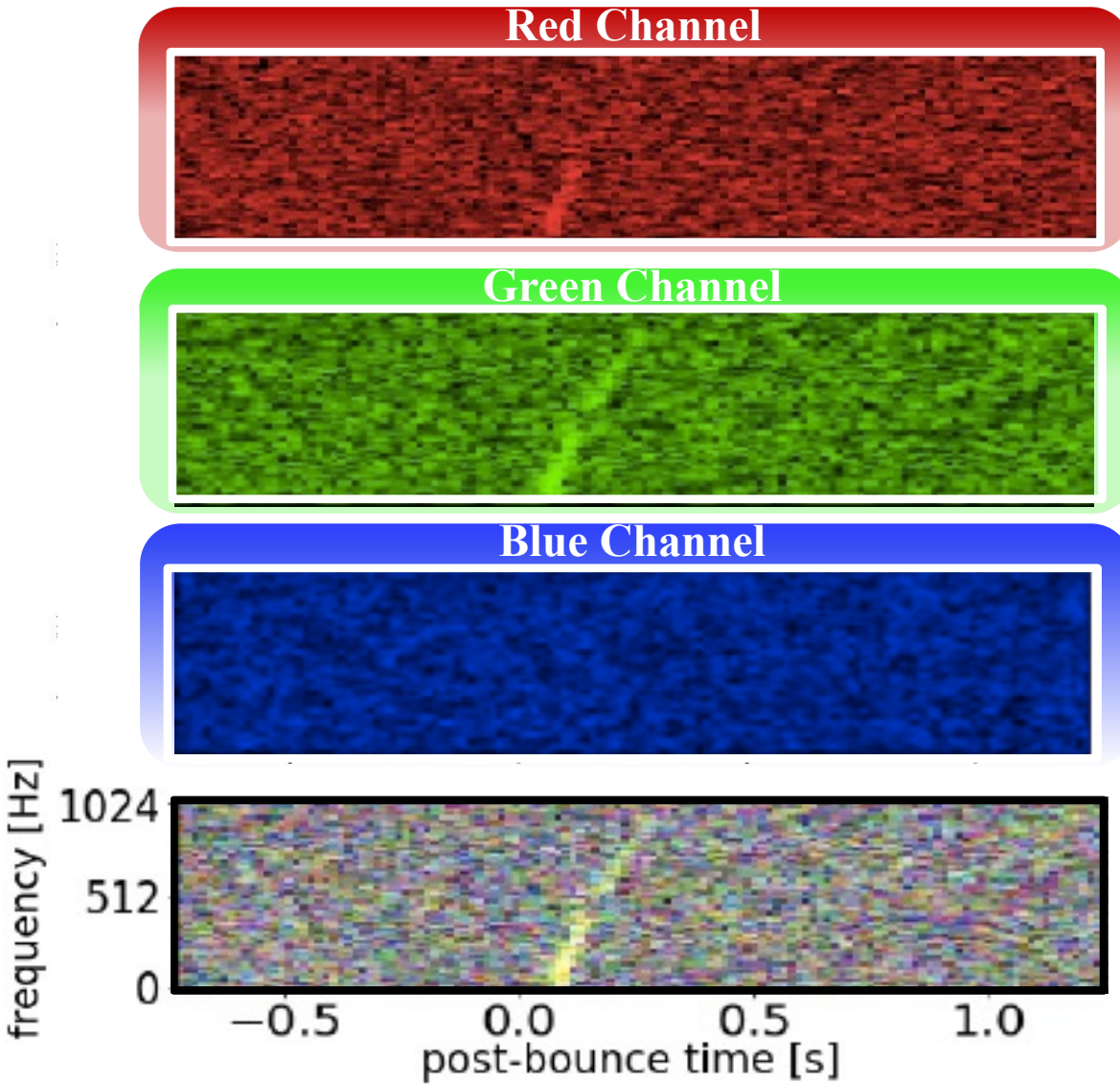
To estimate the model generalization and extrapolation ability it has to be evaluated on previously unseen data, denoted as test set.

Aim of our Convolutional Neural Network

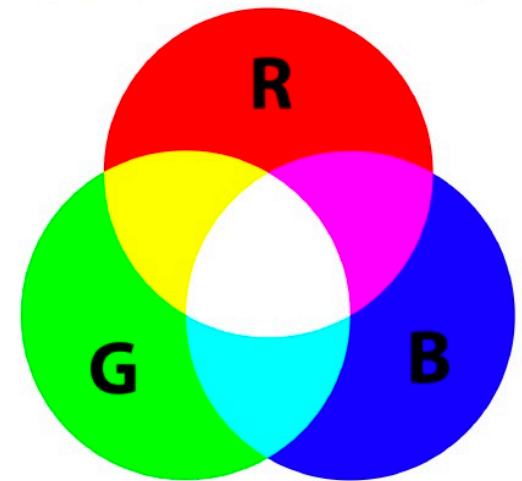
- We want to perform signal detection as an image recognition task, classifying the images in two classes: *Signal* and *Noise*.
- The input images are the RGB multi-detector scalograms, reconstructed using cWB.
- The aim is to build a pipeline for a data-driven weakly-modelled robust search.
- Our RGB approach allows us to straightforwardly exploit coincidences among different detectors.

RGB time-frequency plane

Coincidences among detectors



Additive colour synthesis



LIGO Hanford = red

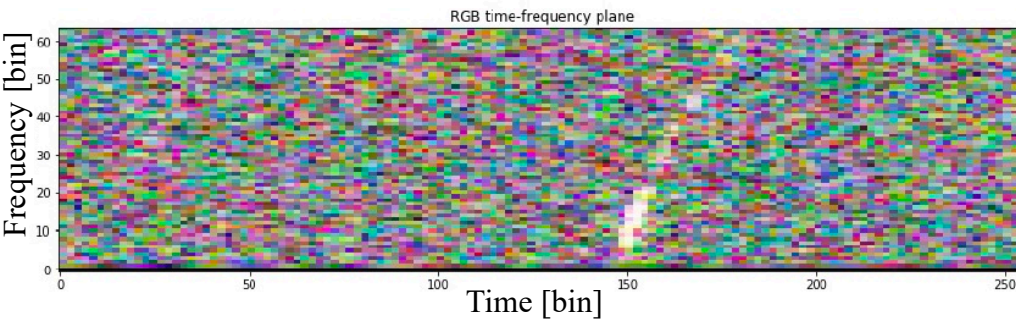
LIGO Livingston = green

Virgo = blue

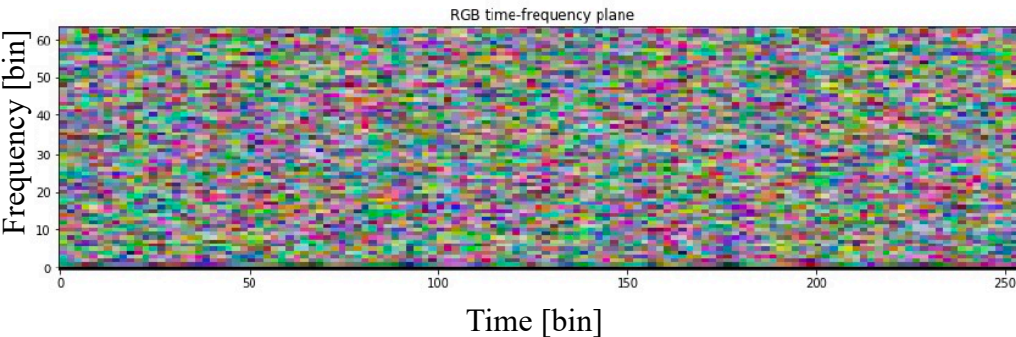
RGB time-frequency plane

Coincidences among detectors

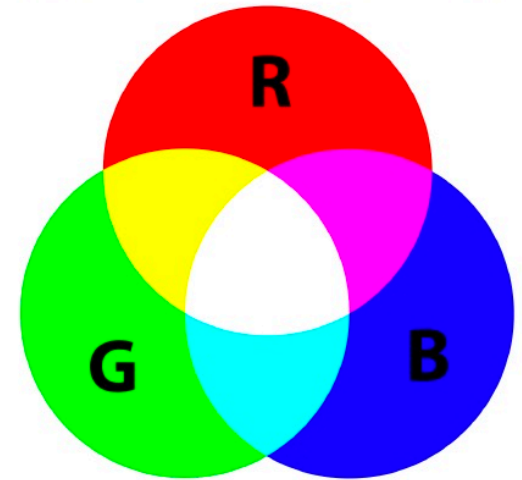
Signal+Noise



Only Noise



Additive colour synthesis



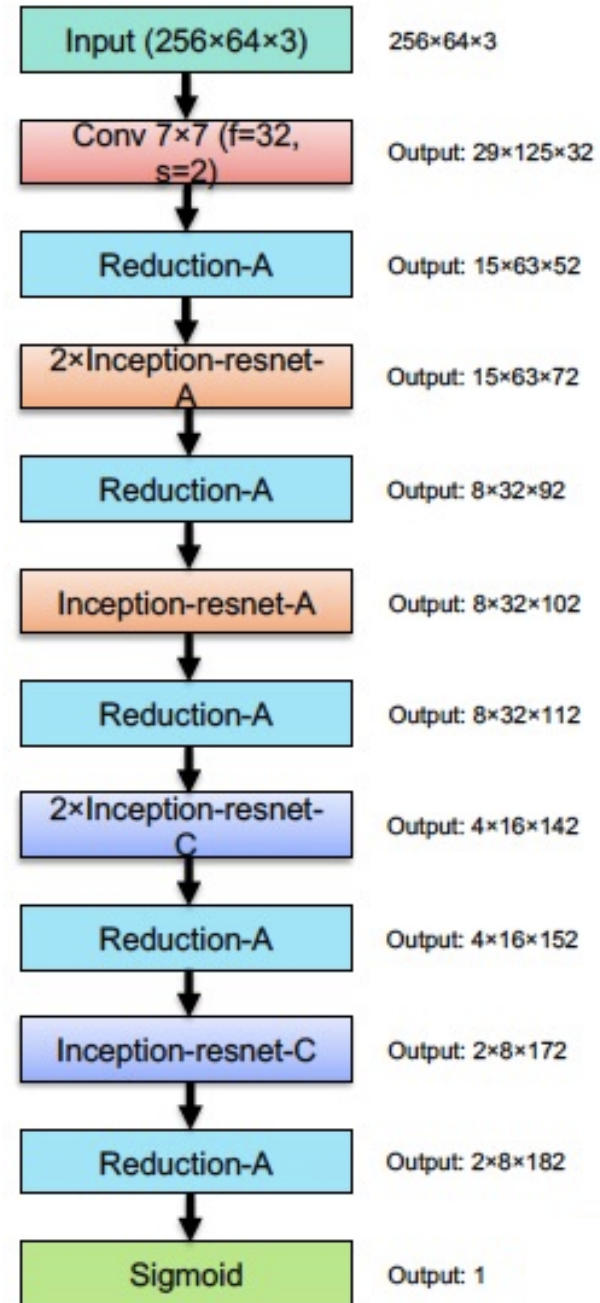
LIGO Hanford = red

LIGO Livingston = green

Virgo = blue

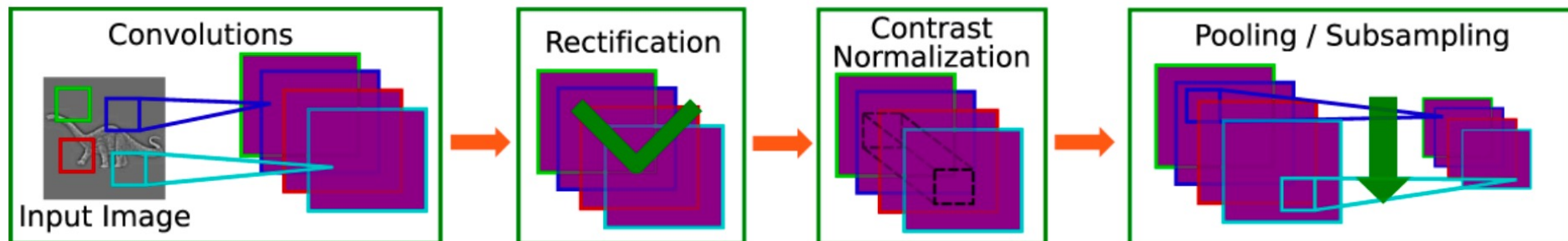
Architecture of the deep learning algorithm

- Mini Inception Resnet v1: reduced version of Inception-Resnet
- Keras framework, based on the TensorFlow backend
- Total number of parameters: 98997
- 30 times more complex than previous network
- The task is treated as a multi-class classification problem with two classes: the event class and the noise class, by using the binary cross entropy.
- The training and validation phase, performed in the real detector noise, is done in 2 h and 21 min using a GPU Nvidia Quadro P5000, while predicting the test set takes 3 ms for each 2 s long image.



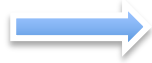
Architecture and training

- Choosing the cWB output at level 6, the single input image (RGB scalogram) is 256x64 pixels x3 (time x frequency x detector), covering the frequency band from 0 to 2048 Hz and a time range of 2s.
- There are 98997 trainable non-independent parameters.
- The training is sequential with decreasing SNR (curriculum learning).



Data: from Gaussian noise to real noise

Gaussian noise



Previous set: 10^4 images for each value of Network SNR $\in [8, 40]$



Phys.Rev. D 98 (2018) 12, 122002

**Real detector noise
(O2 – August 2017)**

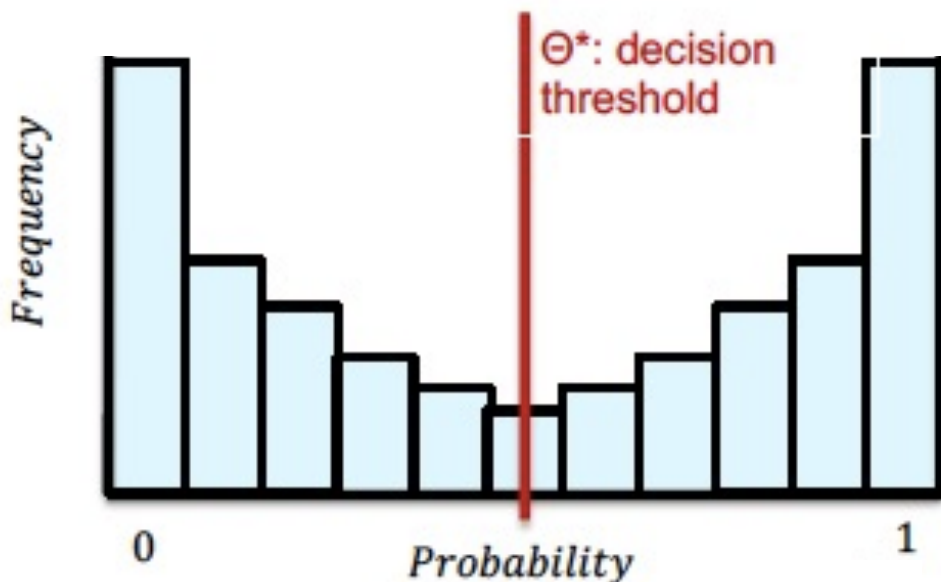
- **Training set – phenomenological waveforms:** 7×10^4 images for each distance $\in [0.2, 3]$ kpc and random sky localisation.
- **Blind set – phenomenological waveforms:** 26×10^4 images with distances chosen in a uniform distribution $\in [0.2, 15]$ kpc. NOT involved in the training or validation procedure.
- **Test set - numerical simulations from the literature:** 6.5×10^4 images with distances $\in [0.1, 15]$ kpc

In particular, we chose a stretch of real data even containing glitches, taken during August 2017, when Virgo joined the run. The period includes about 15 days of coincidence time among the three detectors and we used this data set to generate about 2 years of time-shifts data to train and test the neural network as noise class.



Phys.Rev.D 103 (2021) 6, 063011

Measuring and constraining the learning



Credit: Melissa Lopez

- The output of the network is a probability vector ϑ , which contains the probabilities of the template belonging to one class or another.
- The classification task is performed according to a threshold ϑ^* , the template will be classified as event class only if its probability overcomes ϑ^* .

Confusion matrix

		Actual class	
		Event	Noise
Predicted class	Event	True positive (TP)	False positive (FP)
	Noise	False negative (FN)	True negative (TN)

Efficiency:

$$\eta_{CNN} = \frac{\text{correctly classified signals}}{\text{all the signals at CNN input}} = \frac{TP}{TP + FN}$$

False Alarm Rate:

$$FAR_{CNN} = \frac{\text{misclassified noise}}{\text{all classified events}} = \frac{FP}{FP + TP}$$

False Positive Rate:

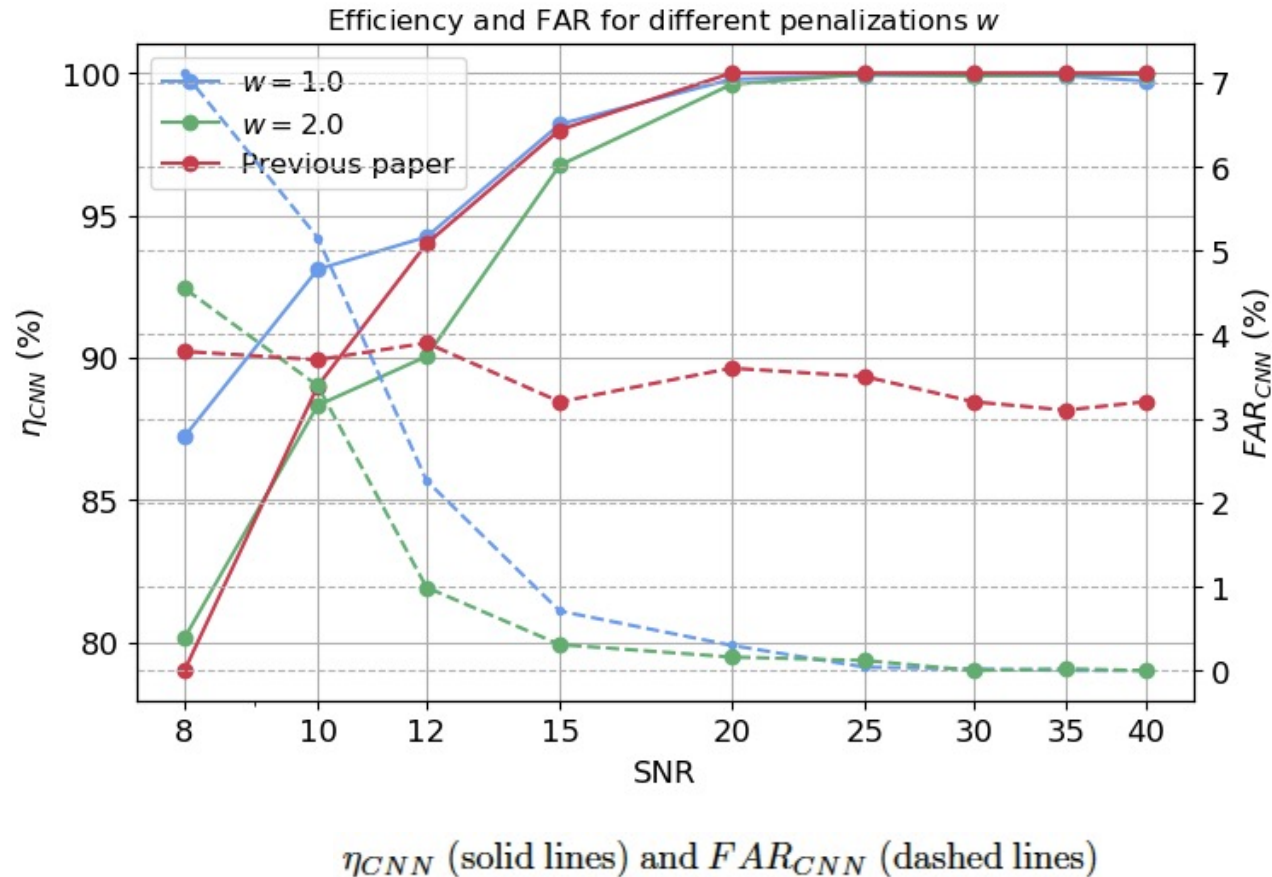
$$FPR = \frac{FP}{FP + TN}$$

Comparison with previous work in Gaussian noise

Weighted binary cross-entropy:

$w=1$ correctly classify the noise class or the event class is the same

$w=2$ it is 2 times more important to correctly classify the noise class rather than the event class.

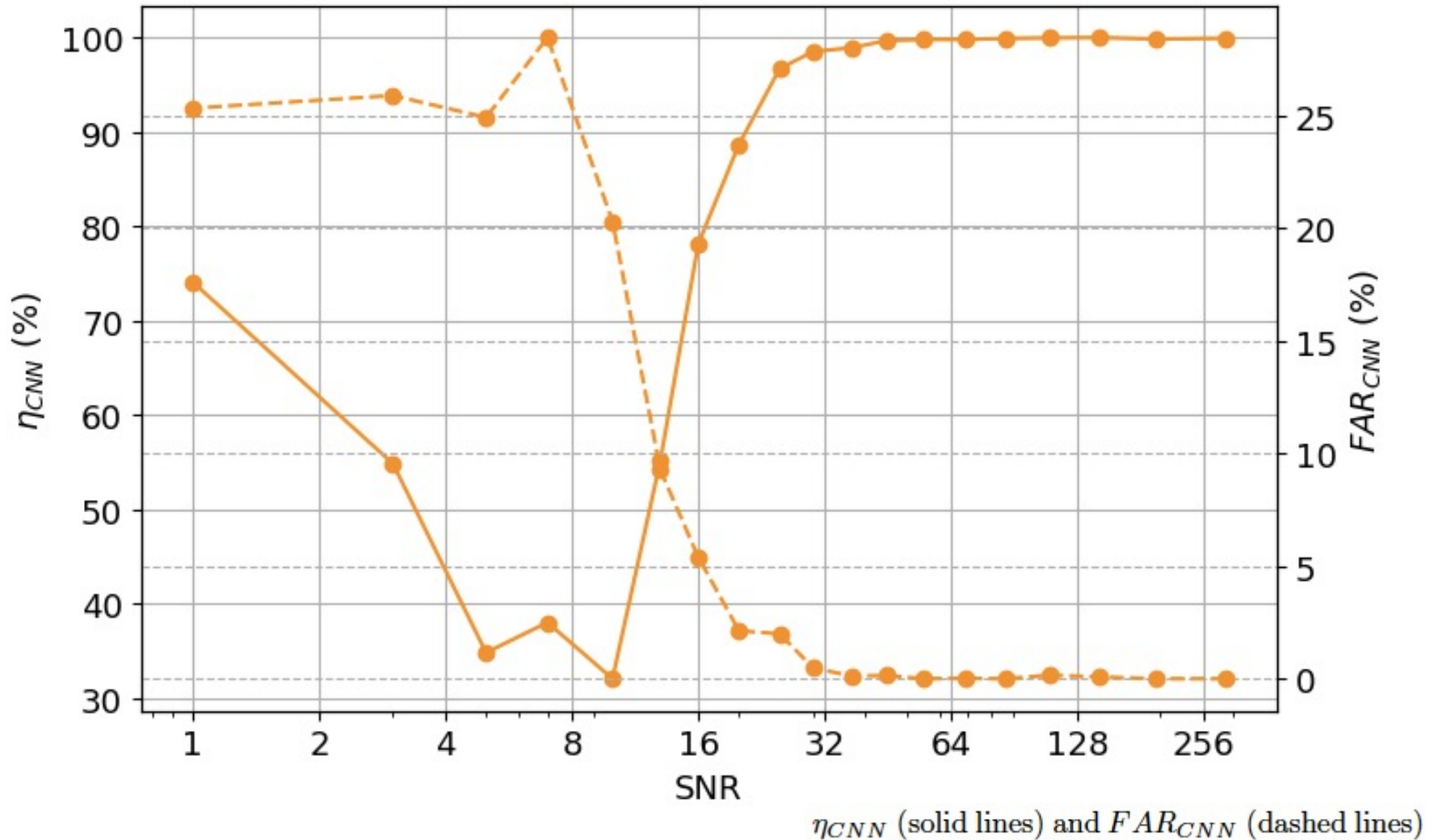


Phys.Rev. D 98 (2018) 12, 122002

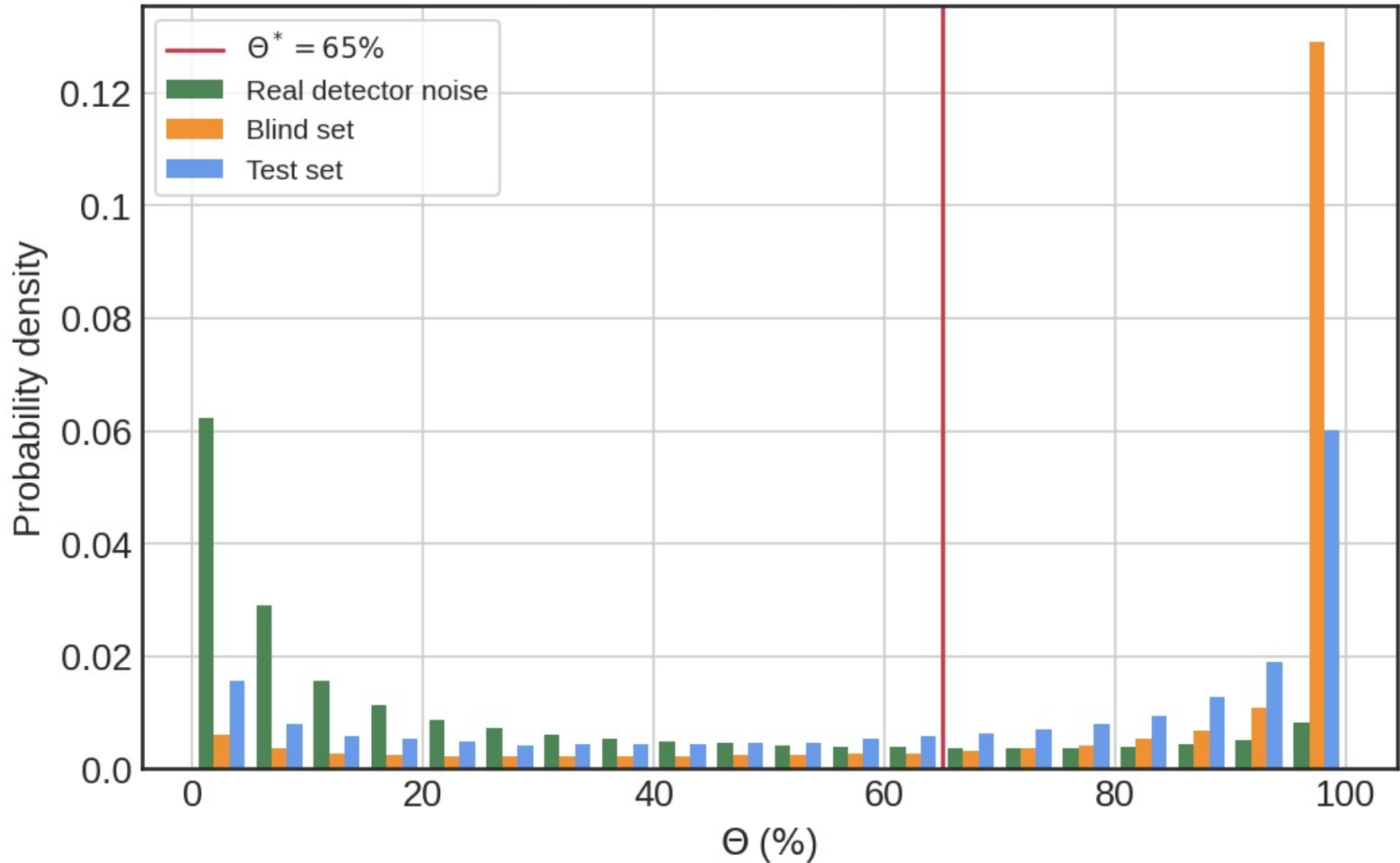


Phys.Rev. D 103 (2021) 6, 063011

Validation process in real detector noise



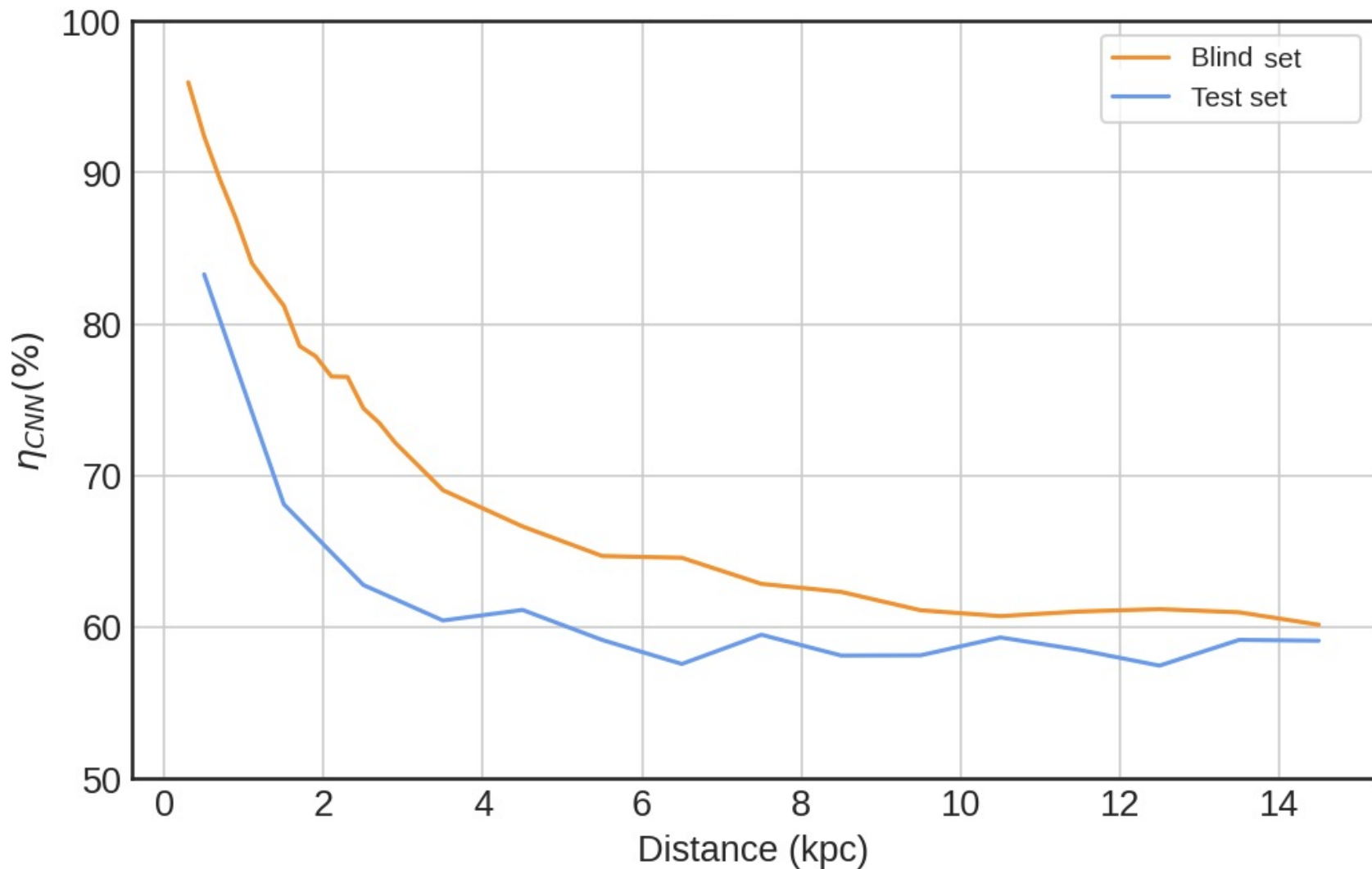
Results in real detector noise



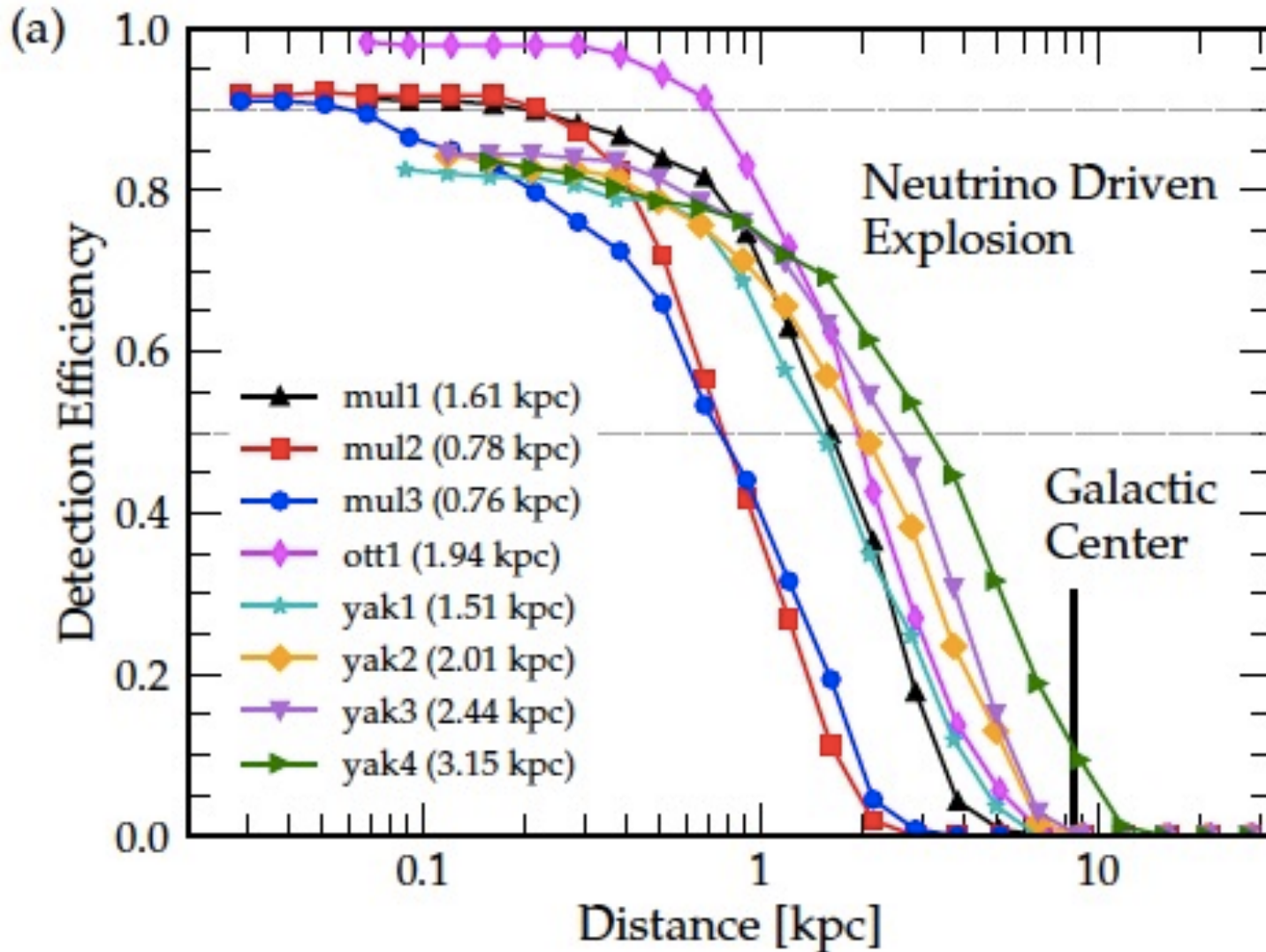
Results in real detector noise

O2 data – network: H1L1V1 – real detector noise

$$\eta_{CNN} = \frac{\text{correctly classified signals}}{\text{all the signals at the input of CNN}}$$

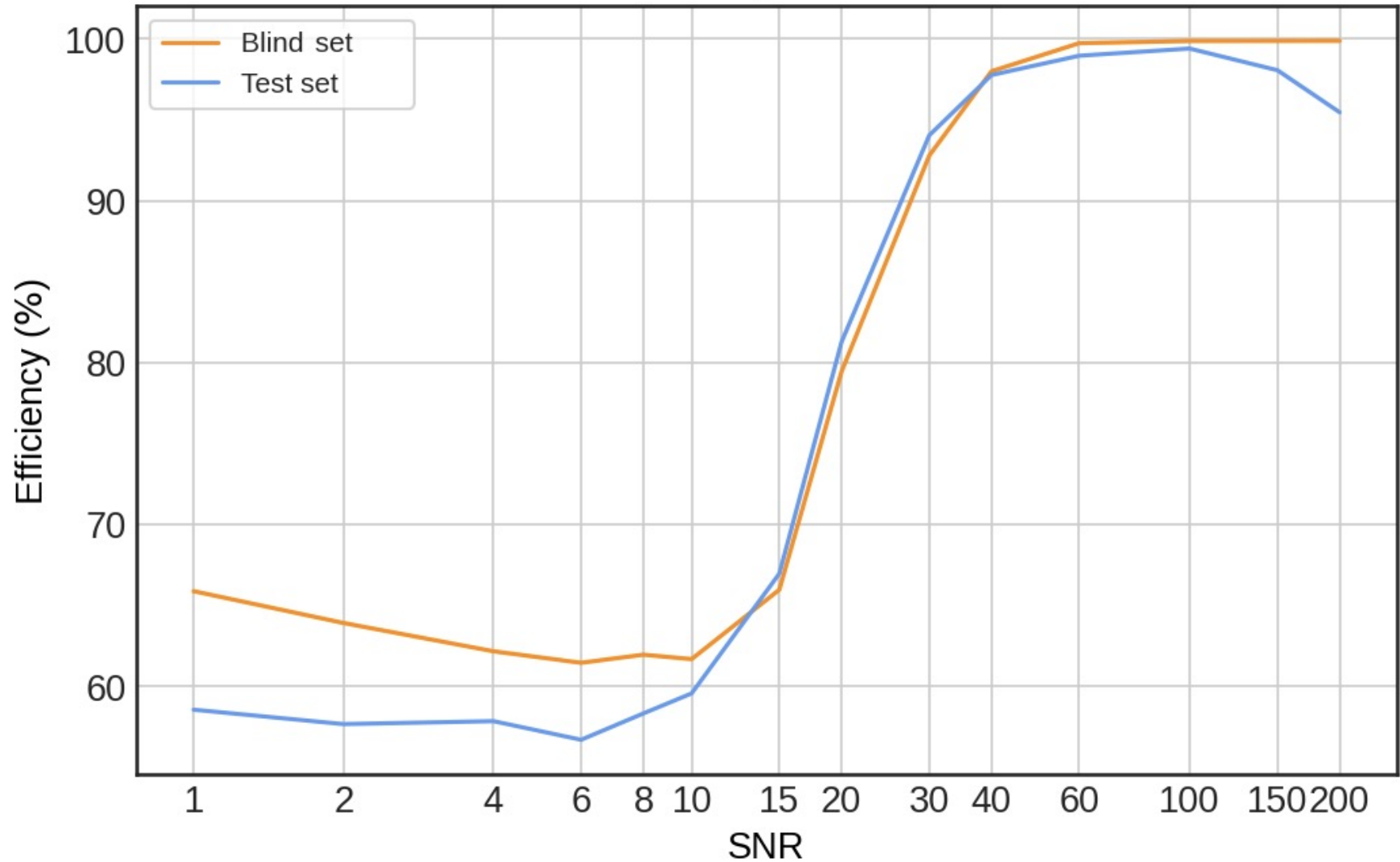


The reference: *Optically targeted search for gravitational waves emitted by core-collapse supernovae during the first and second observing runs of advanced LIGO and advanced Virgo*



Note that the FAR in this search is different from the one discussed in the present talk.

Results in real detector noise



Outline

- What is the astrophysical source we are looking for?
- What are the challenges?
- How do we approach the problem?
- **How can we improve our approach?**

Improvements

- Include the SASI structure in the search
- Consider the rapidly rotating scenario of the magneto-rotationally-driven CCSN
- Enlarge the network of ground-based interferometers including the KAGRA detector

Conclusions

- We trained a newly developed Mini-Inception Resnet neural network using time-frequency images corresponding to injections of simulated phenomenological signals, which mimic the waveforms obtained in 3D numerical simulations of CCSNe.
- In the case of O2 run, it would have been possible to detect signals emitted at 1 kpc of distance, whilst lowering down the efficiency to 60%, the event distance reaches values up to 15 kpc.
- These results are very promising for future detections and the algorithm has multiple possible extensions.

An abstract background featuring vibrant, swirling ink splashes in shades of yellow, orange, red, blue, and green against a white backdrop. The ink forms intricate, fluid patterns that spread across the frame.

THANK YOU
FOR THE ATTENTION

Overflow slides

Waveforms for the test set

TABLE II: List of models of the test set used in the injections. M_{ZAMS} corresponds to the progenitor mass at zero-age in the main sequence (ZAMS). Unless commented, all progenitors have solar metallicity, result in explosions and their GW signal do not show signatures of the standing-shock accretion instability (SASI).

Model name	reference	M_{ZAMS}	comments
s9	[47]	$9M_{\odot}$	Low mass progenitor, low GW amplitude.
s25	[47]	$25M_{\odot}$	Develops SASI.
s13	[47]	$13M_{\odot}$	Non-exploding model.
s18	[48]	$18M_{\odot}$	Higher GW amplitude.
he3.5	[48]	-	Ultra-stripped progenitor ($3.5M_{\odot}$ He core).
SFHx	[49]	$15M_{\odot}$	Non-exploding model. Develops SASI.
mesa20	[50]	$20M_{\odot}$	
mesa20_pert	[50]	$20M_{\odot}$	Same as mesa20, but including perturbations.
s11.2	[31]	$11.2M_{\odot}$	
L15	[28]	$15M_{\odot}$	Simplified neutrino treatment.



[28] T. Kuroda et al., 851(1):62, 2017.

[31] H. Andresen et al., MNRAS 468(2):2032-2051, 03 2017.

[47] D. Radice et al., ApJ 876(1):L9, 4 2019.

[48] J. Powell et al., MNRAS 487(1):1178-1190, 05 2019.

[49] T. Kuroda et al., ApJ 829(1):L14, 9 2016.

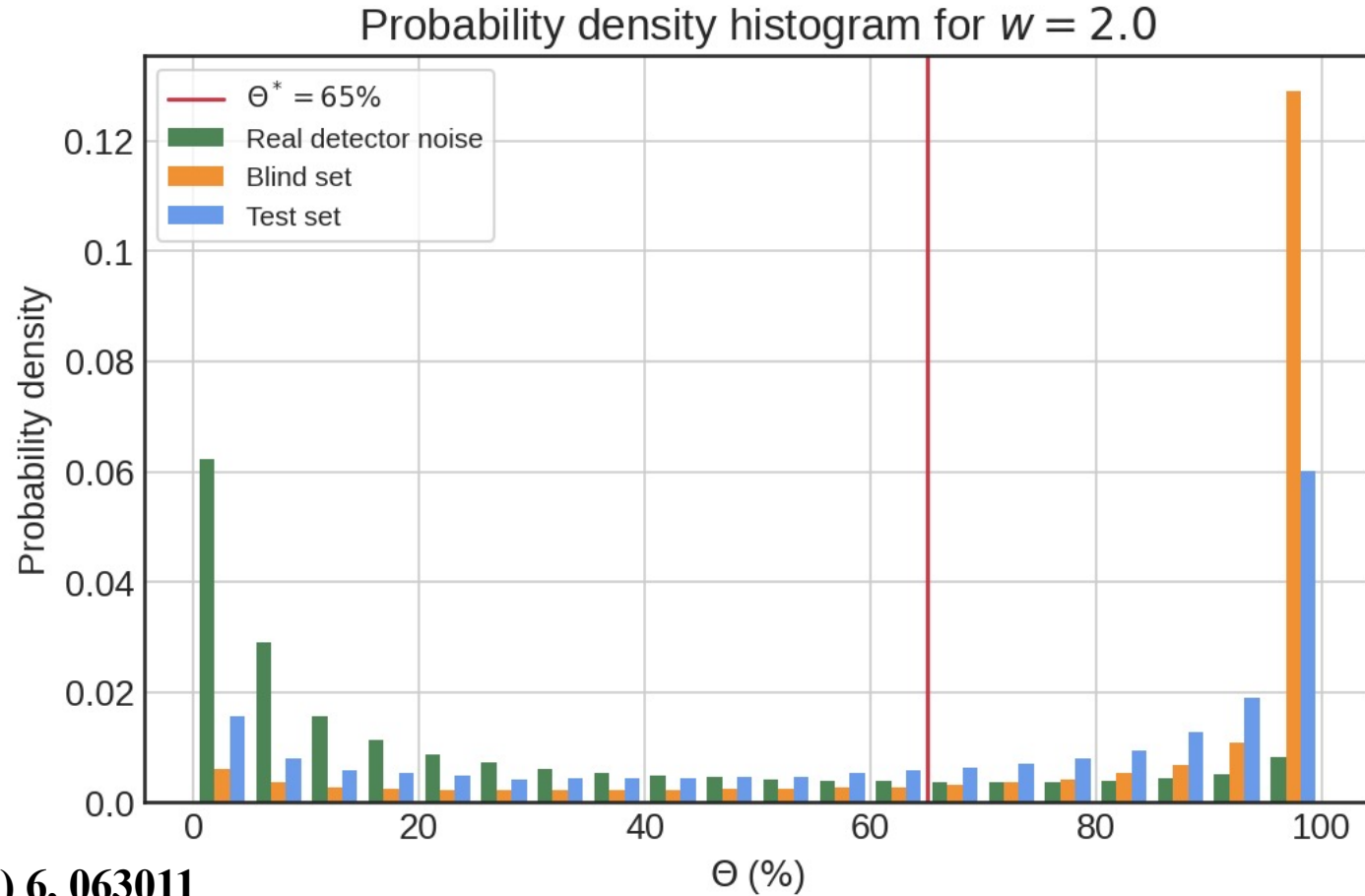
[50] E. O'Connor et al., ApJ 865(2):81, 9 2018.

Results in real O2 detector noise

Given the counts of the i th bin c_i and its width b_i , we define the probability density as

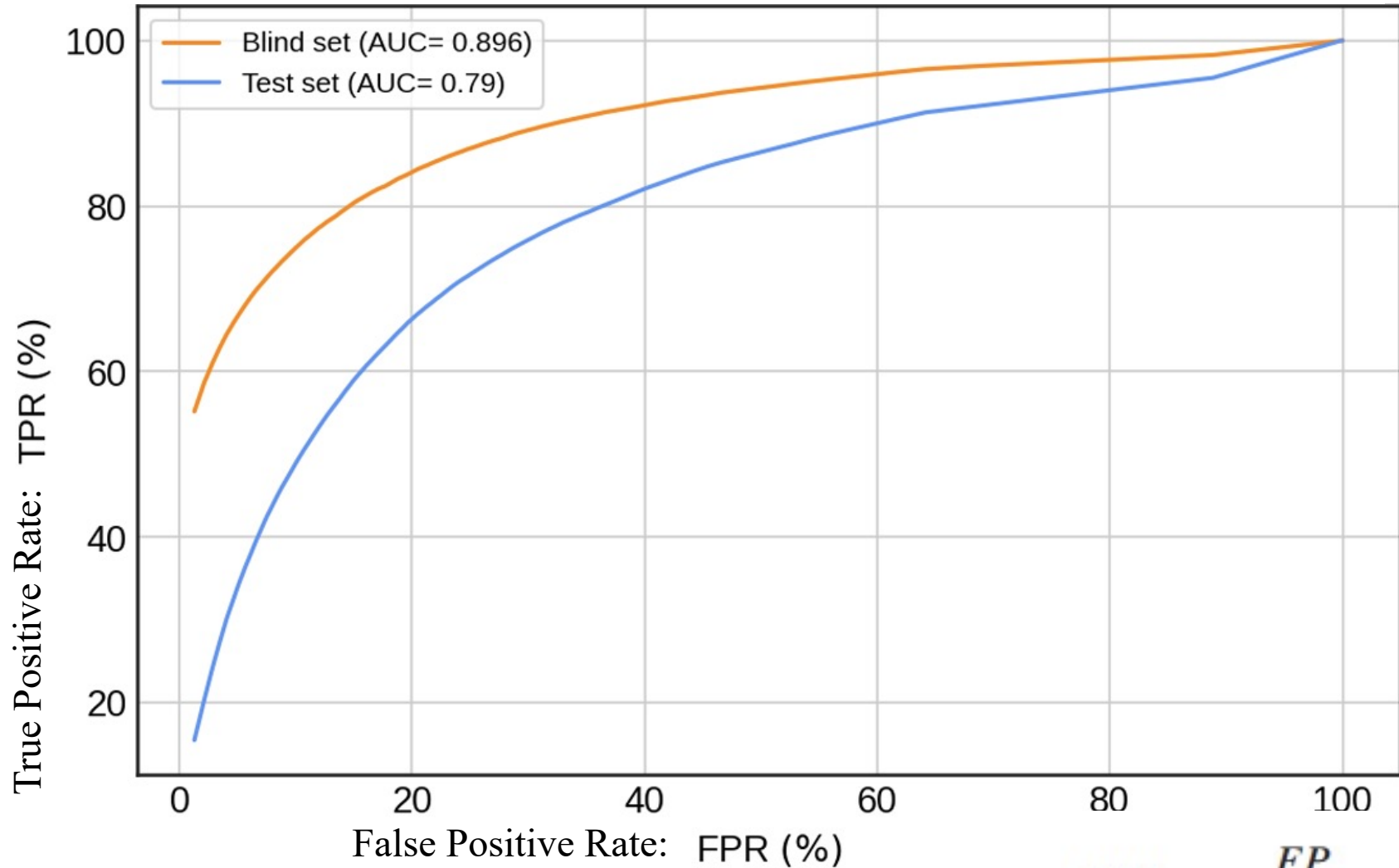
$$c_i / (\sum_i^N c_i \times b_i),$$

where N is the total number of bins of the histogram.



ROC curves

$$\eta_{CNN} = \frac{\text{correctly classified signals}}{\text{all the signals at the input of CNN}} = \text{TPR}$$



$$FPR = \frac{FP}{FP + TN}$$

Previous work

Task: classification problem

Classes: 0 class (noise) and 1 class (event) with different level of noise (SNR)

Learning: curriculum learning

Data: Gaussian noise

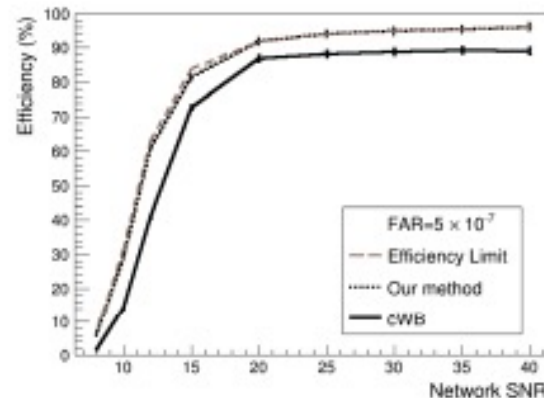
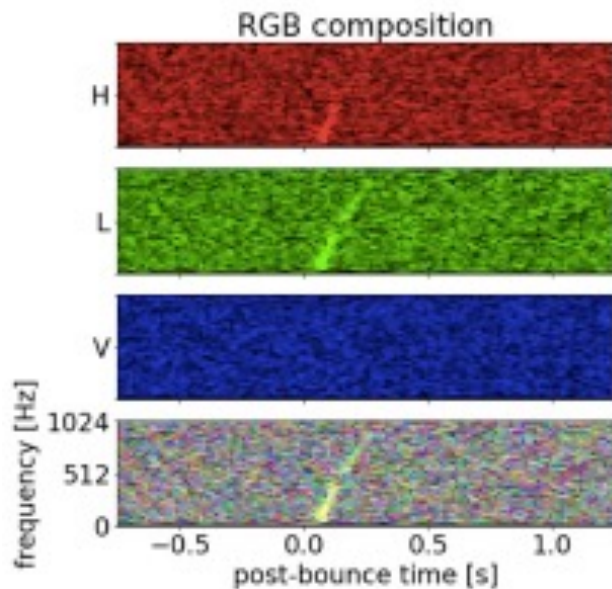


Figure 8: Efficiency vs SNR in the case of complete cW. (continuous) and our method (dashed) for all SNRs. We report also the curve that shows the ratio between the input events of the CNN and the total injected events in function of SNR (brown). This curve sets the maximum efficiency that our method can achieve

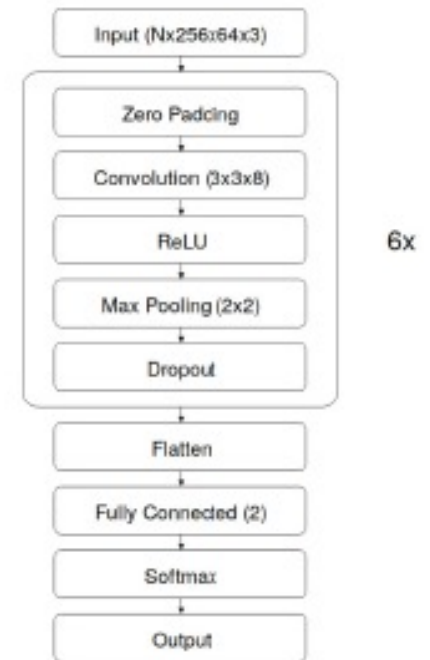


Figure 4: Sketch of the architecture of our model.



Binding energy per nucleon

